An experimental investigation in hard turning of AISI 4140 steel.

A THESIS SUBMITED IN PARTIAL FULFILLMENT

OF THE REQUIRMENT FOR THE DEGREE

OF

Master of technology

In

Mechanical Engineering

By

ABHIJIT SAMANT

Roll No 214ME2549

Under the supervision of

Prof. K.P.Maity

Department of Mechanical Engineering

National Institute of Technology

Rourkela

DEPARTMENT OF MECHANICAL ENGINEERING

National Institute of Technology,

Rourkela, India

National Institute of Technology

Rourkela

C E R T I F I C A T E

This is to certify that the thesis entitled "***An experimental investigation in hard turning of AISI 4140 steel***" submitted by **Mr Abhijit Samant** for the partial fulfillment of requirements for the award of **Master of Technology** in *Mechanical Engineering* with specialization in "**Production Engineering"** at National Institute of Technology, Rourkela is an authentic work carried out by him under my guidance and supervision. To the best of my knowledge the matter embodied in the thesis has not been submitted to any other University for the award of any Degree or Diploma.

Prof. K.P.Maity

Department of Mechanical Engineering

National Institute of Technology

Rourkela

ACKNOWLEDGEMENT

I would like to express my thankfulness to my supervisor **Prof. K.P.Maity** while accomplishing out this thesis to its last frame. I came across a number of people whose commitments in different ways made a difference. It is a pleasure to pass on my appreciation to every one of them. As a matter of first importance, I would like to express my deep sense of regard and special gratitude to my supervisor **Prof. K. P. Maity** for his in valuable guidance consistent inspiration and kind co-operation all through time of work which has been instrumental for this research work.

I am extremely grateful to **Prof. S.S.Mahapatra**, Head of the department, Mechanical Engineering, National Institute of Technology, Rourkela for giving priceless support and permission to use available priceless facilities in the institute.

I would likewise express my gratitude towards **Mr. Asit kumar parida** and **Mr. Swastik Pradhan** (PhD. Scholars) for their consistent help and guidance for the completion of my research work.

I would also like to express my special thanks to **Mr. Rudranarayan Kandi** (M tech Research scholar) for his help and advice throughout the year.

In conclusion, I might want to express my most profound appreciation and admiration to my family member and all my well-wishers, friends and class mates for their backing, tolerance to improve my feelings.

Abhijit Samant
Roll no- 214ME2549
Department of Mechanical Engineering
National Institute of Technology, Rourkela

Abstract

There is a growing demand for new and special alloys like nickel alloys, chrome-molybdenum alloys due to their special properties like high strength, light weight, and corrosive resistance. The present work is stand on the experimental investigation of chrome-molybdenum alloy to study the effect of process parameters like cutting velocity, feed, and depth of cut on the output responses like force, surface roughness, tool wear. A full factorial design with 3^3 lay out with total 27 numbers of runs were carried out and optimum cutting condition for all three output responses was found out using grey relational analysis (GRA) method. White layer formed in a hard turned component is mainly influenced by the abrasive wear of the tool. It has immense response on the performance of product so it is significant to find out the white layer thickness. To investigate the machined surface properties like white layer and micro-hardness, the sliced machined surface was scrutinize under scanning electron microscope (SEM) and micro-hardness tester respectively. It has been found that as the speed increases, the thickness of white layer increases due to increase in flank wear. Finally, a thermo-mechanical 2D model using finite element method available in Deform 2D^{TM} has been prepared to investigate the output responses like force. Further, the model has been validated comparing the results of simulation with the measured results.

Keywords- Chrome-molybdenum alloy, Full factorial, white layer, micro-hardness, Deform 2D^{TM}

Contents

List of Figures

List of Tables

Nomenclatures

Ra	Surface roughness
t_2	Deformed chip thickness
ξ	Chip reduction coefficient
r	Nose radius
λ	Inclination angle
Υ_0	Orthogonal rake angle
ϕ_e	End clearance angle
ϕ	Side clearance angle
α	Auxiliary cutting edge angle
α_0	Principal cutting edge angle
k	Thermal conductivity
α	Thermal Expansion
Cp	Specific heat capacity
ρ	Density
μ	Poisson Ratio
T	Bulk Temperature
Y	Young's modulus
h	Heat transfer coefficient
$\boldsymbol{\varepsilon}_0$	Strain rate
$\boldsymbol{\theta}$	Absolute temperature
$\boldsymbol{\theta}_R$	Room temperature
$\boldsymbol{\theta}_m$	Mean temperature
$\boldsymbol{\tau}$	Frictional stress
$\boldsymbol{\sigma}_n$	Normal stress
HRC	Rockwell Hardness on C scale

Chapter 1

Introduction

1.1 Turning

Turning is a machining operation that produces symmetric parts, by removing unwanted material from a block of metal on a lathe by using single point cutting tool. The work piece which is relatively small compared to its diameter (L/D ratio) is fixed to a rotating axis, and cutting tool is moved across its surface to produce a dimensionally correct member. Frequently machined parts from a pre-shaped work piece are generally cubic or cylindrical in nature, but separately their individual dimensions are quiet complex. Turning is capable to produce different shape of material like conical, tapper, grooved or straight work piece. Research work is carried out to flourish the optimum cutting parameters (speed, feed, depth of cut) for each group of materials through the years.

1.2 Hard Turning

Hard turning is characterized as a machining process performed on hardened steel and cast iron component (concerns hardness value over 45 HRC) by using a single point cutting tool on a rigid and accurate machine [1]. Increased demands for improved productivity and cost efficiency have driven the hard turning process to a new level. The arrival of super hard cutting tool material such as cubic boron nitride (CBN), polycrystalline diamond (PCD) and polycrystalline cubic boron nitride (PCBN) is well accepted cutting tool material for hard turning to meet industry productivity goals of higher quality and shorter cycle time [3]. The material which are routinely hard turned are steel alloys, bearing steels, high speed steel, die steel, case hardened steel and heat treatable powered metallurgical part. It is emerged impressively in various machining operation such as milling, boring, broaching, hobbing etc. [9].

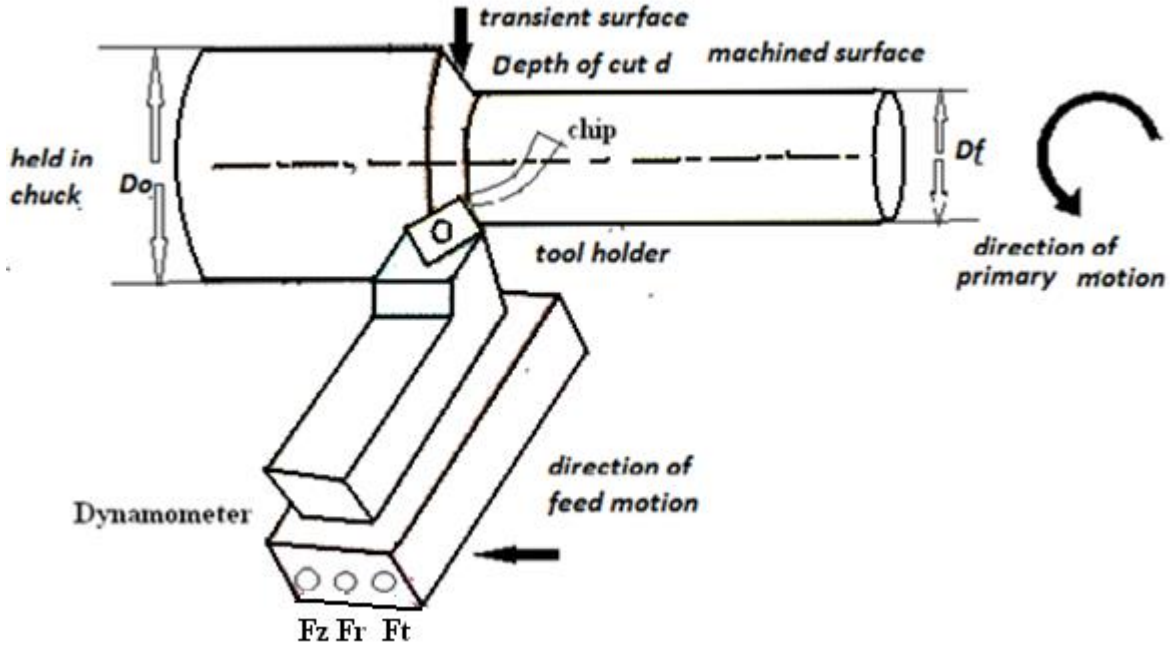

Figure 1 Schematic diagram of turning operation

Hard turning is generally used in industry to eliminate the grinding operation for finishing a part. Machine tool requirement in case of hard turning is more rigid and accurate to achieve a quality surface. The surface finish ranges from 0.4 to 0.8 micrometer, roundness and diameter tolerances about 2-5 micron and +/- (3-7) respectively can be achieved with an appropriate hard turning process [5]. The (L/D) ratio should be less i.e. it should not be more than 4:1 for an unsupported work piece. The level of accuracy and precision in a hard turning component is generally characterized by the degree of system rigidity, which minimized the extension of tool, overhang of the work piece and extension of machine tool part. The main challenge in hard turning process is whether or not to use coolant. It is better to perform hard turning on dry condition [7], because for interrupted cuts (in gears) the cutting tool experienced with thermal shock which is a reasonable cause of tool failure. Generally, low concentrated water based coolant used during the hard turning operation [40]. The behavior of the chips such as glowing orange and flow like ribbon during continuous cut show the overall idea about machining condition.

1.3 Hard turning different from conventional turning

Hard turning is different from conventional machining in various ways, to implement hard turning successfully in industry we should know the differences very clearly.

- The machine tool requirement in case of hard turning should be more rigid and accurate to get a better surface finish.
- The shear angle is very small in case of hard turning and with increasing hardness of work piece material shear angle increases simultaneously.
- Thrust force is a dominant cutting force which is greater than tangential cutting force in case of hard turning, with increasing the flank wears the differences get larger between these two forces.
- In a hard turning operation a saw tooth type of chip is formed due to the fractured of work piece material in their shear range.
- In hard machining the compression ratio of chip is tends to equal to 2.
- The tangential and radial component of force is mainly depends upon the rake angle of the tool. In case of zero rake angles these components do not increase with increase in hardness of material.

1.4 Industrial application and limitation

Hard turning has several potential advantages over grinding. In automotive industry hard turning is especially competitive to improve the manufacturing quality and productivity [14]. It also used in automotive industry for semi finishing and finishing operation of transmission shaft, engine components, and axel. To produce gears, landing struts and components of aerospace engine hard turning is considered as a primary machining operation performed in air craft industries. A major practice of hard turning process was in bearing industry [15] to reduce the production step such as heat treatment and grinding.

All over the world Manufacturers always make progress toward lower cost solution. In gear manufacturing industry four grinding steps were used to prepare a surface like A B and C and chamfer edge which can be reduced to one step and minimize the production cost about 60% [24] with the help of a one-step hard turning set up.

Hard turning have a major advantage over grinding such as the operation can be done at faster rate on one setup. It allows more flexibility to perform an operation than grinding. [4] Most of the operation can be performed at one clamping like rough and finishing operation at CNC lathe. Multiple turning operations can execute easily on an automated lathe. The most crucial advantage is that hard turning can be operated in dry condition which reduces the coolant cost and its disposal.

1.5 Factors influencing hard turning

Hard turning is roughly defined as an operation of removing material from the work piece using a machine tool to structure it into a proposed design. Research is going on for more than a century for better understanding on machining process. Parts which are usually hard turned from a pre-shaped work piece are typically cubic or cylindrical in their overall shape, but their individual features may be quiet complex. It is considered as one of the vital and most accurate process in manufacturing industry due to high tolerance and surface finish. The innovation of NC technology and its application to machining made the process capable to produce complex 3D surface [30].

- Properties of work piece material

The work piece properties play a vital role to affect the machinability criteria in hard turning. Most influencing properties are microstructure of the material, nature of the work piece material, thermal conductivity and mechanical and chemical properties of the material.

- Material and geometry of the cutting tool

Geometry and material of cutting tool are also influencing the machining process. Now a days different types of cutting tool material used in practice for hard turning operation such as high carbon steel, cemented carbide, ceramic and sintered oxides, cermet, cubic boron nitride,(CBN) polycrystalline cubic boron nitride, (PCBN) etc. Different types of coating of various layers on cutting tool insert also influenced the cutting tool life. Geometry of the cutting tool which control the hard turning operation are given below

- Rake angle
- Clearance angle
- Cutting angle
- Inclination angle
- Nose radius of the tool

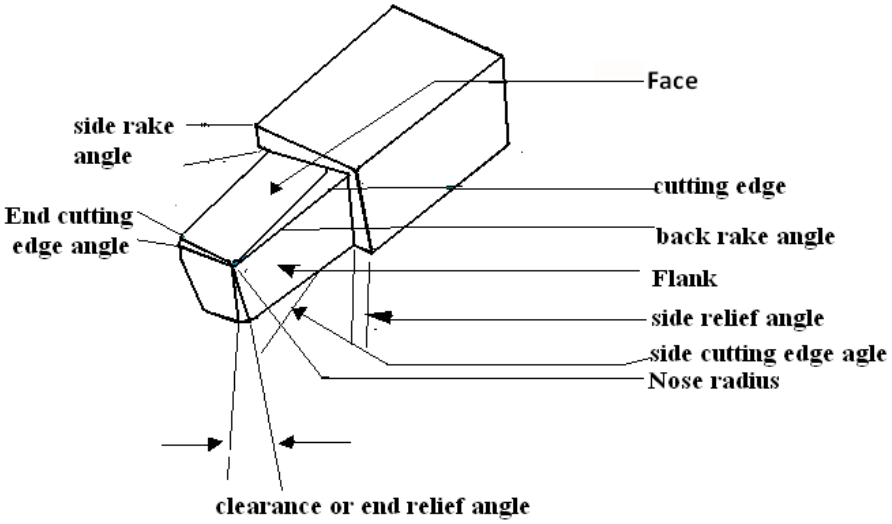

Figure 2 Cutting tool geometry

➢ Cutting parameters

To perform an effective turning proper cutting parameters have to be selected.The different types of cutting parameters that mostly influenced the cutting are described below.

- Cutting speed (N) It is defined by the rotation of the spindle in one minute The maximum diameter of the work piece (to which tool is exposing for machining) is always taken to calculate the speed.
- Feed velocity (f) It is specified as the velocity with which the machine tool is travelling along the work piece.
- Depth of cut (d) It is the depth by which tool is penetrating into the work piece.

- Machining environment

Hard turning was always preferred to perform on a dry condition.

1.6 Cutting force

The forces induced during the metal cutting operation are acted upon tool. (Shown in figure 3) The knowledge of forces and its behavior is important to estimate the power requirement and design of the machine tool. The cutting forces will vary with the variation of cutting speed, tool angle, composition of work piece, tool material and use of cutting fluid.

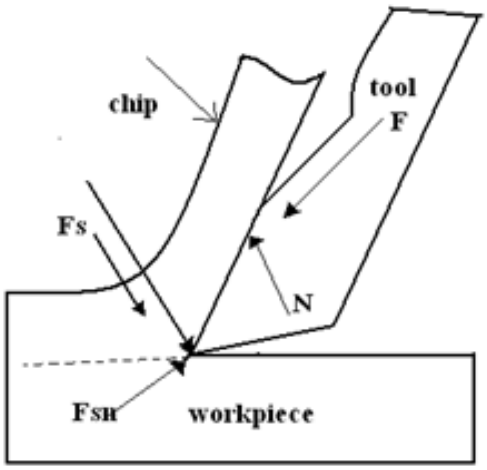

Figure 3 Cutting force on tool

F- is the force acting due to frictional resistance of the tool acting on the chip. This force act downwards against this as chip glides along the tool face.

N- Indicates the action on the chip which is normal to the frictional force.

Fs- Shows the resistance to the shear of the material in forming the chip. This force acts along the shear plane.

Fsn- This is normal to the shear plane and is called backing of force provided by the work piece on the chip.

1.6.1 Merchant's theory

Most of the research work on machining (since 1930) is carried out on the basic of plasticity theory. Then the study of chip morphology comes into pictures where the main objective is to optimize the cutting force, temperatures and stresses involved in the process. Various techniques were adopted to study the fundamental of cutting process by analytical method, but most convenient and simplified model is introduced by Merchant (Merchant 1945). He developed the model by establishing the relationship between the measurable and actual forces by a circle known as Merchant's circle.

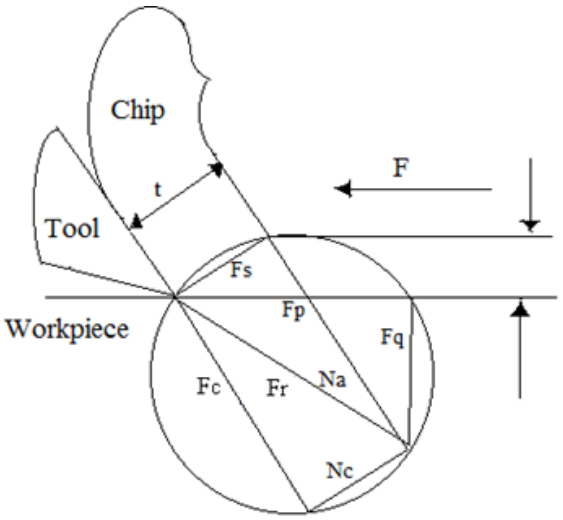

Figure 4 Merchant's orthogonal cutting model

F_s Component on shear plane

F_p Cutting force

F_c Frictional force

F_q Thrust force

F_r Resultant force

N_c Normal to the rake face

N_a Normal to shear plane

In this case while the cutting action takes place the work piece revolving at a constant speed while the cutting tool remains stationary in its original place. During the cutting action the formation of chips takes place which is rigid in nature and it is in equilibrium under the action of force in chip tool interfaces and across shear plane. Along the tool chip interface the resultant force Fr is transmitted. According to the figure 4 Fr has two components on shear plane and rake face. The components acted on the shear plane are called Fs and the force which is normal to the shear plane is called Ns. The other two forces namely Fp and Fq are acted on the cutting direction and normal to the work piece respectively. The force Nc is acting normal to rake face. Whereas the force Fc is acting in

the chip flow direction. The following equation represents the relation between the components and their resultant on the shear plane.

$$\begin{bmatrix} Fs \\ Ns \end{bmatrix} = \begin{bmatrix} \cos\phi & -\sin\phi \\ \sin\phi & \cos\phi \end{bmatrix} \begin{bmatrix} Fp \\ Fq \end{bmatrix} \qquad 1.1)$$

$$\begin{bmatrix} Fc \\ Nc \end{bmatrix} = \begin{bmatrix} \sin\alpha & \cos\alpha \\ \cos\alpha & -\sin\alpha \end{bmatrix} \begin{bmatrix} Fp \\ Fq \end{bmatrix} \qquad (1.2)$$

Shear angle ∅ can be determined by

$$\phi = \tan^{-1}\left(\frac{t_u \cos\alpha}{t_c - t_u \sin\alpha} \right) \qquad (1.3)$$

1.6.2 Slip line field theory

This theory approaches plastic deformation in plane strain for a rigid plastic body. The approach is largely adopted for Finite Element Modeling. For shear angle slip line field is established based on two assumptions.

(i) The material cuts shows the characteristic like an ideal plastic, where the strain harden property generally not found.

(ii) The maximum stress is found in the direction of shear plane.

A slip line field ABC in front of the cutting tool, shown in figure 5 was behaved like rigid plastic which sustain uniform state of stress.

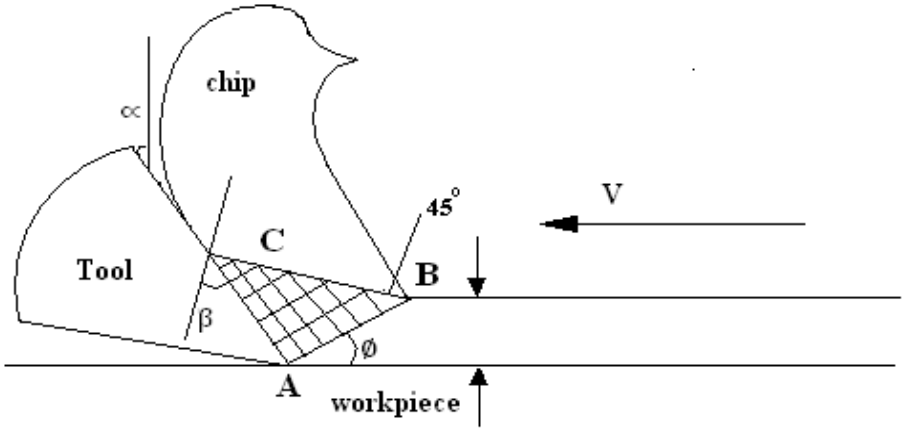

Figure 5 Slip line field in orthogonal cutting

The stress is zero along the line BC. The angle on the rake face is termed as friction angle (β) and the shear angle Ø can be evaluated by following equation.

$\beta = \tan^{-1}(Fc/Nc)$ (1.4)

$\emptyset = 45^0 - \beta + \alpha$ (1.5)

1.7 Tool wears in hard turning

Tool life is one of the most important and widely used criteria in case of hard turning. During the turning process cutting tool experienced consistent heating due to tool chip friction and shear deformation energy. There are different modes of tool failure.

(a) Plastic deformation failure

Due to the wrong selection of process parameters and tool materials the cutting tool tip experience greater temperature than the hot hardness temperature of the tool material. Because of this temperature, the tool wear takes place at a faster rate and the tip of the tool deformed plastically.

(b) Gradual wear failure

In this type, tool is wearing out gradually and whenever the wear becomes considerable, it can't perform satisfactorily. It is taking place due to crater and flank wear.

- Crater wear- The crater (a shallow spherical depression present on surface) is formed on the tool rake surface due to diffusion and adhesion of small chip particles flowing over it. The major tendency of this failure is due to the abrasion between the tool face and chip. Most commonly it was seen during the turning of titanium alloy.
- Flank wear-It takes place on the tool's flank face . The main reason of this type of tool failure is due to the friction at tool interface and the abrasive action of the microchip at tool work interface. The formation of wear land is not in a continuous form. It was most commonly seen during the hard turning where chemical affinity is very low.

(c) Diffusion wear- The presence of atomic attraction between atoms of the work piece and tool, the tool material atoms are diffusing from the tool end depositing over the work piece, which is known as diffusion wear.

1.8 Surface roughness

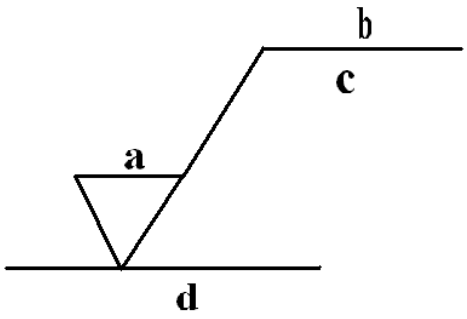

a=roughness value (Ra)

b=production method

c=sampling length

d=direction of lay

Surface roughness expresses the state of machined surface. It determines the surface topography, which is essential to confirm surface suitability for its function. The size of irregularities on a machined surface have extensively influence on the condition and quality of end product [9]. Measuring surface roughness suggests that assessing them by their peak, depth and distance. Then the analysis was done by a proposed method and estimated as per industrial standard. Surface roughness can be indicated in various process

such as average roughness or center line average (Ra), Root mean square average (RMS),maximum peak (R_Y),ten point roughness (R_Z),. Out of them most normally utilize for surface roughness is R_a. It is characterize as an average of the absolute assessment of the profile height alteration from the mean line. R_a is the average of a set of individual measurement of a surface peak and valley. It is also called as center line average (CLA).

Specification of surface texture:

Surface texture- The small deviation from the real geometry of an actual surface is called as surface texture Shown in Figure 6 which is remain on the surface at regular or irregular interval leads to form a pattern or texture.

Roughness-It is generally characterized as a short wavelength due to the tool marks and individual scratch. Such marks produced by a single traverse of a planning tool.

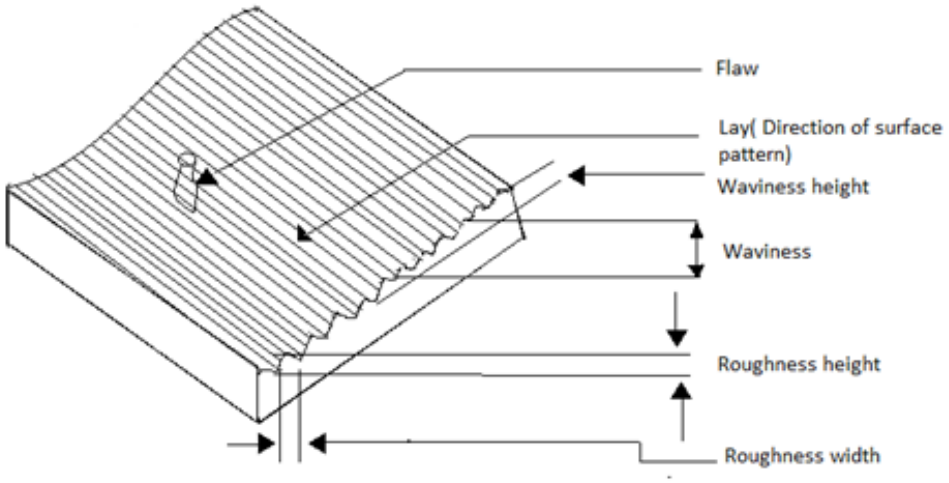

Figure 6 Surface topography of a machined surface

Lay- The lay is the tool or scratch marks taken collectively which characterizes the particular process. Where these show definite directional characteristics as for example, in planing operation this is called the lay of the surface.

Waviness-Waviness is the longer wavelength irregularities upon which roughness is super imposed. Waviness may be induced by vibration, hard spots, imperfect turning of a grinding wheel, chatter, heat treatment etc.

1.8.1 Magnitudes usually measured in surface finish

1. Average roughness (Ra)or ten point height of irregularities (Rz)
2. Maximum peak to valley height (Rt)
3. RMS value of Roughness (Rmax)
4. Average over definite ordinates
5. Form factor
6. Bearing area

1.8.2 Maximum peak to valley height

Though the surface A and B have the same Rt value, we cannot say that both are of the same roughness value. Hence this is not a satisfactory measure of roughness. In addition the value of Rt if interpreted in the wider sense, it means that the peak and valley would almost certainly be exceptional and the value obtained would not give a representative assessment of the surface.

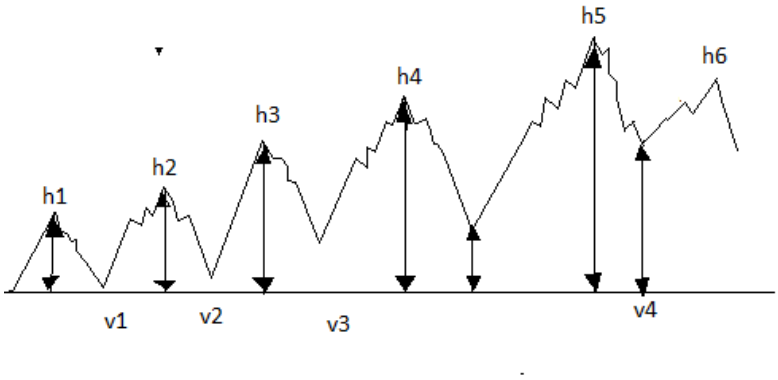

Figure 7 Ten point average method

In spite of the draw backs, Rt is a satisfactory measure in cases where it is desired to control the cost of finishing for checking rough machining. This method is advantageous in cases where the condition of surface is likely to exert an important influence on such

properties as fatigue resistance. To overcome this lack of representation the 10 point average Rz, (shown in Figure 7) is used which is determined as follows:

$$Rz = \left[\frac{(h_1 + h_2 + h_3 + h_4 + h_5) - (v_1 + v_2 + v_3 + v_4 + v_5)}{5} \right] * \left(\frac{1000}{vm} \right) \quad \text{.....(1.6)}$$

VM=vertical magnification, h1, h2, h3 are max peaks (in mm), v_1, v_2, v_3.are valley's

Average roughnesses:

This is also called 'Centre Line Average' (CLA) and denoted by Ra

$$R_a = \frac{(A1 + A2 + A3 + ...An)}{L} \quad (1.7)$$

$$R_a = \frac{(\sum A)}{L} \quad (1.8)$$

Where, L=sample length, A=Total area

$$R_a = \frac{(|h_1| + |h_2| + |h_3| + ... + |h_n|)}{n \times \left(\frac{1000}{v.m} \right)} \mu m \quad (1.9)$$

$$R_a = (\frac{(\sum |h|)}{n} \times \frac{1000}{VM} \mu m \quad (1.10)$$

$$R_a = \left(\frac{1}{L} \right) \int_0^L h dL \quad (1.11)$$

To determine average roughness value by erection ordinate is a laborious process, however irregular area is divided by its length and each area can be measured by using plain meter. So Ra value has found greater favor of measure.

There are fundamentally two techniques by which we can describe the nature of a machined surface

- Qualitative method- In this method no instrument is used to specify surface roughness but to know the condition of a surface visual inspection and touching is required.
- Quantitative method- This method makes use of instruments to get a quantitative estimation of the surface quality to be measured, These are
  - Wallace surface dynamometer
  - Tomlinson surface meter
  - A Piezo electric instrument
  - Moving coil type instrument
  - Surface profilograph
  - Talysurf

1.9 Chip formation mechanism in hard turning

Hard turning is virtually a material removal process, used to produce a desired shape and size with a high dimensional accuracy and surface finish. In this process the unwanted material is removed from a block of metal in the form of chip. The chips possess different types and patterns, which are mainly due to the variable condition of machining environment, tool geometry, and work piece material. The pattern of chip and its characteristic such as size, shape and color present a better idea about machinability of work piece, level of cutting temperature, condition of cutting edge, impact of machining parameters and function of cutting fluid in a machining process.

1.9.1 Mechanism

The chips are formed due to shearing (ductile material) and brittle fracture (brittle material) action in machining process. The force is applied on the work piece by using the tip of cutting tool. Material is started deforming plastically and sliding over the rake face of the tool inducing shear stress on the layer of the work piece material [14]., at a point the induced shear stress will become larger than the ultimate shear stress of the work piece material. Then shearing and cracking is taking place at the tip of the tool and its propagating towards the surface of the work piece.

During the machining of soft and ductile materials because of higher toughness the crack wave propagation will absorbed by the material and disappearing somewhere in the middle, so that continuous chips will be produced [20].

Whereas during machining of hard work piece because of lower toughness the energy wave can propagate very easily to the surface so that discontinuous chips are formed.

1.9.2 Types of chip

- Continuous chip- These types of chips are usually produced when cutting ductile materials such as low carbon steel, aluminum and copper. It is severely deformed either in the form of a long strip or crul into a tied roll shown in Figure8**,** and in contact with the tool face for a longer period of time resulting in more frictional heat. These are avoided by using a chip breaker.

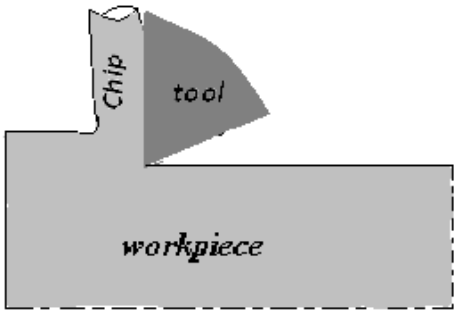

Figure 8 Continuous chip

- Discontinuous chip-It is obtained due to lack of ductility necessary for appreciable plastic chips formation shown in Figure 9. The material ahead of the tool edge fails in a brittle fracture manner along the shear zone. It is generally produced by cutting grey cast iron, bronze and hard brass.

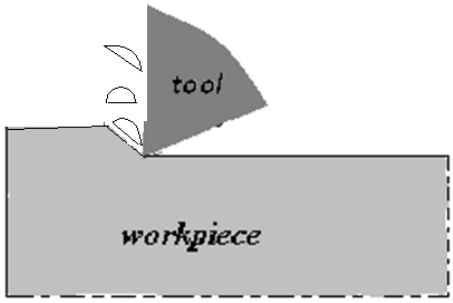

Figure 9 Discontinuous chip

- Segmented chip- This type of chips also obtained during the machining of hard material, shown in Figure 10, but it is also obtained during cutting the ductile material at a very low speed, small rake angle and by using the cutting fluid.

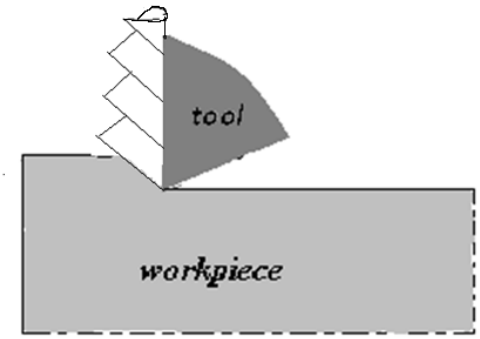

Figure 10 Segmented chips

1.10 White layer

White layer is found on a machined surface due to the microstructural alternation. It is labeled “white” layer because it can able to prevent the common etchants and appeared white under an optical microscope. [8] Further the hardness of white layer is more than bulk material. White layers are hard and fragile and commonly associated with a tensile stress which affects the quality of a machined surface [2]. It is generated in case of many engineering application. The generation of white layers can be divided into three main categories. Firstly white layers are generated at various manufacturing process such as grinding, turning, drilling, rimming, milling and blanking. Secondly it can be found on the surface of various used engineering components such as railheads, piston rings. Thirdly white layers can be generated in laboratory by experimental method. Generally white layers have been associated with grinding because relative heat flow in the work piece surface is significantly higher in grinding than normal cutting because of poor heat transfer properties of the grinding wheel [6] such as aluminum oxides.

1.10.1 Mechanism of Formation

There are generally three mechanisms which mainly responsible for white layer formation.

The mechanism of plastic flow .Which produces a homogeneous structure or with a fine grain structure. The mechanism of rapid heating and quenching which results in transformation products. The mechanism of surface reaction with environment such as nitriding, carburizing.

The first two mechanisms are difficult to separate and may depend on each other .For example phase transformation temperature may be affected by plastic strain or strain rate. Thickness of white layers occurs on the surface of a steel may be up to 10 micro m thick [7]. The dark layer present underneath it may be two to three times thicker than white layers. It was observed that white layer possess a Nano crystalline structure under the Scanning Electron Microscope and Optical Microscope due to large strain deformation and dynamic recrystallization.

Chapter-2

Literature review

2.1 Effect of cutting parameters on force.

H.V. Ravindra et al. (1993) proposed an analytical form to characterize the time of tool wear and wear force relationship for turning operation. In turning operation cutting force have a measure impact on progressive wear and tool failure. The measurement of the wear of the tool is essential to optimize the process control so tool wear is generally associated with the measurement of the force, current, vibration and temperature. The result reveal that force components is a better indicator of wear process and it also eradicate variation in material properties which is a major source of noise in signal measured during machining. Experiment was designed to obtain the data for establish a relationship among cutting condition on cutting forces and tool wear. The author also claims that an effective on line monitoring and control can be done by using these models.

Manjunatha et al. (2015) reviewed the response of process parameters on performance characteristic like tangential force, feed force, surface roughness and flank wear by machining EN-19 steel with uncoated carbide insert. The research work was performed based on Taguchi's L_{27} orthogonal array under dry cutting condition, whereas for flank wear L_9 orthogonal array was used. The result revealed that depth of cut was an influential parameter of both tangential and feed force and surface texture. Flank wear mostly affected by feed rate and cutting speed.

Souad Makhfi et al. (2013) investigated to develop a robust numerical model to predict the force in hard turning process. In this paper Artificial Neural Network (ANN) was proposed to forecast the cutting force components by hard turning of AISI 52100 bearing steel with the help of CBN tools. This research based on experimental data measured during hard turning. Speed, feed, doc and hardness of work material was taken as input parameters in ANN model whereas cutting force components are output parameters.

During the study which uses BR/LM algorithm and a single hidden layer noted that on 6 tested conditions MAPE ranges from 0 to 36% on 18 cutting force components database, and no more double hidden layer take advantage over single hidden layer. The various type of transfer function was studied and various numbers of neurons in hidden layer have been tested.

Zoltan Iosif Korka et al. (2013) studied the most important parameters of machining process i.e. cutting forces. Experiments were carried out on a SN 560 type lathe. Work piece material was mild steel and tool was HSS with a 25 mm square shank. Cutting forces was estimated theoretically with the help of ($F_I=C_F*f*t$) this equation and experimentally with the help of 9257B (KISTLER) type dynamometer. It would be concluded from the theoretical and experimental result that among three cutting parameters feed rate is mostly affect the cutting forces. Mathematical model suggested the influence of cutting parameters on cutting forces.

Li Qian et al. considered the response of cutting forces of high speed orthogonal machining on a hard turning process. Numerical simulations were carried out to determine cutting forces and feed forces. Properties of the work piece materials for simulations were assumed. The experiments were conducted on AISI 52100 bearing steel, AISI H 13 hot work tool steel, AISI D2 cold work steel, AISI 4340 alloy steels with the help of CBN or PCBN inserts, for hard turning Feed force measured as higher than cutting forces. The cutting forces and feed forces increase with increasing of feed, nose radius, rake angle and hardness of work piece. The conclusion is compared with other research work for consistency.

G. Harinath Gowd et al (2012) investigated to predict a mathematical model for calculating feed force, cutting force, thrust force and surface roughness. Speed, feed, doc significantly affect feed force, thrust force and cutting force in turning operation so in present research these are recognize as decision making variables. The objective was found out by performing experiment on INCONEL 600 and Response surface methodology (RSM) used to anticipate a numerical model. After perform the experiment it was set that, feed force (Fx), thrust force (Fy), cutting force (Fz) and surface roughness are established by using a second order polynomial model.

S.R. Chauhan et al. (2012) Investigated the performance of polycrystalline diamond (PCD) cutting insert for turning titanium (Grade-5) alloy by using Response Surface Methodology. The machining parameters such as cutting speed, feed, and depth of cut have been considered in investigations. The surface roughness and tangential forces are the response variable. The experimental plan is based on face centered CCD. Experimental result indicates that surface roughness increase with increase in the cutting speed and feed rate. The tangential force increases with increase in approach angle and depth of cut. The results of ANOVA and the conducting confirmation test prove that surface roughness and tangential force predicted values close to 95% to experimental value.

2.2 **Effect of cutting parameters on white layer**

Ian S Harrison (2004) investigated to figure out whether either Barkhausen sensor or electrochemical impedance spectroscopy technique are viable to distinguish white layer non-destructively. Experiments were carried out on AISI 52100 steel bars with the help of CBN cutting insert on a hard turned lathe. Experimental result shows that Barkhausen sensor is not strongly co-related with white layer. Electrochemical impedance spectroscopy shows a promising result as a method for detect white layer by study the frequency response of a part with or without a white layer .Barkhausen sensor measured by taking five different locations on each part. He also examined the electrochemical properties of white layer defect by electrochemical impedance spectroscopy. The white layer measurements are compared with the output from the Barkhausen sensor and the electrochemical tests to check whether are effective to detect white layer effectively.

D Umbrello et al. (2009) studied to build up an advance method for flow stress and describe the white and dark layer structure to execute in a FE code. AISI 52100 was taken as work piece material. The specimens were prepared as disks of 150mm diameter and 2.5mm thickness. Orthogonal turning were conducted on CNC lathe using CBN 100 inserts. Piezoelectric dynamometer and an infrared thermo camera were used to recognize the local temperature. Simulative and experimental results reported that the changes occur in formation of white layer i.e. increasing with the cutting speed in contrast dark layer

decreases because of heat affected zone (HAZ) and corresponding temperature. A good understanding achieved between experimental and numerical result, which shows that there was an impact of cutting parameters on white and dark layer formation, and that was the white layer increases with increase in cutting speed, feed rate and interestingly dark layer decreases.

Aramcharoen et al. (2008) investigated the benefits of coating on surface hardening in conventional and high speed machining. He was performed the machining of H13 tool steel by using CrTiALN, CrTiAln+MoST and uncoated carbide tools as tool materials. The study shows that formation of white layers at cutting speed 200m/min were 33%, 36%, 41% harder than the bulk material for respective tool materials.

G Bartarya et al. (2014) investigated to study the effect of cutting parameters on white layer thickness, hardness profile and the surface finish produced. The research work was performed by analyze the turning of AISI 52100 grade steel by using uncoated Cubic Boron Nitride (CBN) insert with predefined flank wear. The experiments were performed for various cutting speed and tool flank wear values. It could be concluded that white layer thickness can be controlled by selecting suitable cutting speed even when machined with worn out tool, by reducing the cutting speed 195m/min to 123m/min reduction of white layer thickness reduced by 67%. White layer produced.

A Ramesh et al. (2005) investigated the difference in properties and structure of white layer produced at the time of machining of AISI 52100 steel at different cutting speed. The experimental work including Transmission Electron Microscope (TEM), X -ray diffraction (XRD) and Nano indentation are used to detect the white layer. TEM results recommend that white layer creates at low and medium cutting speed due to grain refinement and white layer observed at high cutting speed is due to temperature. Residual stress profile acknowledged a trend to increase tensile stress with increased thermal effect at work piece surface. This shows that at high machining speed thermal load on a work piece surface is higher. Nano indentation result delivers common information about that by increasing cutting speed hardness of white layer increases.

G. Poulachon et al. (2005) examined the development of white layers created during continuous tool flank wear in hard turning with CBN tools, and compare it with the surface roughness of machined surface. The following four materials $X160C_rM_oV12$ cold work steel (AISI D2), $X38C_rM_oV5$ hot work steel (AISI H11), 35NiCrMo16 high toughness steel and 100Cr6 bearing steel (AISI 52100) are used as work piece material on this study Chips were metallographically prepared and inspect under the electronic microscope to detect if white layers are present or not. More specifically chip structure was studied to decide how they behave with appearance of white layers. Finally by using scanning electron microscopy and EDS technique on this chip samples, properties and microstructures of white layers were derived in order to verify some of the previous theories.

S.S. Bosheh et al. (2006) measured the negative response of white layers on surface finish and fatigue strength of the products. Experiments were done by CNC MHP lathe machine on H13 tool steel bar. The machining was performed using CBN insert. Temperature was measured by pyrometer during machining and white layers depth were analyzed by using Scanning Electron Microscope .Finally flank and crater wear area were also investigated. The study conducted showed that the depth of hardness of white layer reduced at higher cutting speed and hardness gradually reduced from machined surface to bulk material.

M.C. Shaw et al. (1998) investigated the mechanism of chip formation on hardened steel by turning with polycrystalline cubic boron nitride insert. They studied the chip width with various cutting ratio by machining titanium alloy and hard steel with respective cutting condition. Considerable experimental evidence supported their result that saw tooth chip is cyclic cracks developed at free surface of work piece. Chip speed causes the temperature rise due to which austenite formation took place in material, and the formation of white layer affect tool face friction between the work piece and tool.

2.3 **Finite Element Analysis (FEA)**

Chen Zhuo et al. (2015) analyzed the effect of depth of cut on cutting forces by machining a titanium based alloy. In this research work Finite Element Method (FEM) software, DEFORM- 3D used to simulate cutting process of materials and to validate the simulation experiments were carried out to determine the cutting forces. The result of above research work give a conclusion that DEFORM- 3D shows a good accuracy on predicted cutting force value.

Ibrahim A. AI-Zker (2007) studied the fundamental of hard turning process and the impact of CBN tool edge preparation and cutting condition on hard turning variables, chip morphology, temperature and residual stresses. A two dimensional (FEM) model was used to understand overall study. He also carried out a compression test to obtain the data for machining simulations. This compression test provides flow stress data with good predictions. He also predicted the cutting tool edge geometry by using finite element method and the result showed that maximum von-Mises stress on a cutting insert possess the smallest value.

Dong Min Kim (2015) Investigated to reduce the friction of tool- chip interface using textured tool rake surface. The technique was modeled in simulation using DEFORM software package. Perpendicular, parallel and rectangular textured pattern were used in his investigation. A conclusion drawn from his research that perpendicular pattern at an effective edge distance of 100μm pitch size of 100μm and pattern height of 50μm produced lowest force value.

Y. Huang et al. (2002) investigated the response of thermal property of the cutting tool on cutting forces. They modify Oxley's machining theory by analytical approach of the thermal behavior of primary and secondary heat sources. As well as modified Johnson-Cook equation is used in Oxley's approach to establish the relation between material properties with strain, strain rate, temperature. The experiments were done by hard turning AISI H13 tool steel with low and high CBN content tools. Lower thrust force, tangential force and higher tool-chip interface were predicted by both the proposed model and finite

element method (FEM) during the use of lower CBN content tools. The study also show that Johnson- Cook equation behave better within the normal machining condition.

Yung-Chang Yen et al. summarized the response of different cutting tool edge (round, chamfer) on formation of chip, cutting forces and cutting variables in orthogonal cutting as find out by FEM simulation. The Lagarangian thermos- viscoplastic cutting simulation was used to obtain the steady chip flow and cutting forces. Tool temperature and stress was predicted on tool rake face and the behavior of the material at the proximity of the edge radius defined by location of stagnation point. Based on the simulation result an engineering analysis was performed to analyze tool geometry and tool wear Additionally the tool edge geometry optimized in terms of minimum tool wear for given cutting condition.

2.4 **Hard turning**

S Abdul Kalam et al. (2015) studied the effect of gas cooling system during hard turning. Experiments were done on machining hardened D3 steel by chamfered CBN tool. They used SEM and FESEM for surface topography and EDAX technique for phase study. The experiments were performed under dry and gas cooling condition. White layer was seen by cutting 2.5 mm thickness and etched with nital sol^{n} for ten second. They studied the depth of white layer at different cutting speed. The work shows that 80% argon and 20% co_2 as a shield gas for D_3 steel eliminated the white layer.

Salvi et al. (2013) investigated to find out optimum cutting condition by hard turning on 20MnCr5 steel in a CNC lathe machine by using ceramic based TNGA 160404 cutting insert to obtain a better surface finish. The experiment was designed by using Taguchi method and an orthogonal array, the signal to noise ratio and analysis of variance (ANOVA) were used to investigate the cutting characteristics. The experimental result suggested that feed rate followed by cutting speed played a significant role to produce lower surface roughness. The measured Ra value lies between 0.91 to 6.37μm.

B Fndies et al. (2010) investigated to figured out a statistical model of surface roughness in hard turning of high alloy steel X38CrMo5-1 of hardness 50 HRC with the help of

CC650 (chemical composition 70% Al2O3+30%TiC) insert. Experiments were conducted under dry condition based on 3^3 full factorial designs i.e. a total of 27 experiments were done. Minitab software was used to analyze mathematical model concerning the effect of main cutting variable such as speed, feed and doc on cutting force components. Finally the result gives a conclusion that feed rate is the influential factor followed by cutting speed and depth of cut to get better surface finish.

M Remadna et al. (2006) developed a methodology to determine descriptive parameters during machining of hard material alloyed steel (52HRC) by cubic boron nitride (CBN) insert. A large part of this paper aim to correlate between wear and direction of cutting force during machining. Experimental result shows that cutting force increases gradually by increasing cutting distance and tool flank wear. A specific study carried out for forces shows the direction and module of force which is generated by machining. The result also shows that inserts have better orientation of force during starting time. Surface finish obtained by machining has a greater geometrical advantage and the state of machined surface are hard to control because they are linked to a cutting geometry that evolves considerably in the course of insert lifetime.

2.5 **Hard turning on AISI 4140**

Saeed et al. (2009) carried out hard turning operation on AISI 4140 using CBN cutting insert to determine the effect of hardness and spindle speed on surface roughness. A multiple regression analysis using analysis of variance conducted to determine the performance of experimental value. Modeling work was done by using Artificial Neural Network (ANN) and regression method. Experimental data for surface roughness compared with predicted data to show the preference of ANN to determine surface roughness.

Ashar et al. (2015) carried out an experimental study on a chromium-molybdenum alloy steel having hardness (58 HRC) by using L27 orthogonal array design. The time of cut was 3 minute for each run of experiment and the output responses were surface roughness. This study concluded that by increasing depth of cut from 0.3 to 0.5 surface roughness

decreases but from 0.5 to 1 it increases. From ANOVA table it is clear that feed and depth of cut are important factors for surface roughness.

Ilhan Asilturk et al. (2011) carried out an experimental study to optimize the turning parameters based on Taguchi method (L_9) to reduce surface roughness value by machining AISI 4140 (51 HRC) with coated carbide tools. Each experiment was carried out three times with a new cutting insert to measure accurate reading of surface roughness. Signal to noise ratio (SNR) and analysis of variance (ANOVA) are applied to study the effect of speed, feed, and doc on surface roughness. Variance analysis was applied signal to noise ratio to understand the relation between cutting parameters and Ra and Rz value. The studies revealed that feed rate most significantly affect Ra and Rz value. In addition the two factor interaction between feed rate-cutting speed and depth of cut- cutting speed were appeared to be most important.

Aslan et al. (2006) performed an experimental study to measure the flank wear and surface roughness on machining AISI 4140 (63 HRC) steel with Al_2O_3 + TiCN mixed ceramic insert. Experimental analysis i.e. combined effect of three cutting parameters on two performance measure were done by using orthogonal array and analysis of variance (ANOVA) and experimental study was managed by using Taguchi technique. In this study multiple linear regressions was used to determine the relationship between cutting parameters and performance measure. The above experimental analysis gives a conclusion that cutting speed affect significantly on tool wear i.e. if cutting speed increases then tool wear decreases. The optimum value of cutting speed and depth of cut are 250 m/min and 0.25 to 0.50 mm respectively. The two interactions, cutting speed - feed rate and feed rate – depth of cut have a significant influence on surface roughness. Finally the result encourages using Taguchi parameters to obtain optimal cutting parameters for ceramic tool.

2.6 **Design of experiment**

M. Dhanenthiran et al. (2016) studied the effect of process parameters in turning operation on cast iron by using titanium carbide insert. They resolved the results based on factor like machining time, surface roughness, tool wear, material removal rate. Experiments were conducted by varying the speed, depth of cut and feed and the design was based on L18 orthogonal array. Graphs are plotted by using design expert software. Based on this research it was concluded that machining of cast iron using titanium carbide insert gives better results like less surface roughness, high material removal rate and low tool wear. A Multiple linear regression model was developed by using experimental data to optimize the cutting condition in turning operation.

M. Kaladhar et al. (2010) performed the study to optimize machining parameters in turning of AISI 202 austenitic stainless steel using CVD coated cemented carbide inserts. They performed the experiments by using full factorial design in design experiment (DOE) on a CNC lathe. The influence of process parameters during machining were analyzed by analysis of variance (ANOVA). From above experimental work it was observed that feed rate followed by nose radius significantly affect surface roughness. A significant inclination was noticed between speed and nose radius to influence surface roughness. And finally it was observed that measured value and predicted values are closer to each other. ((1444)))

Aveek Mohanty et al. (2014) concentrated on the impact of various process variable of EDM, for example peak current (Ip), duty factor (Tau) and pulse on duration (Ton) on various performance characteristics like material removal rate(MRR), surface roughness(SR), radial overcut(ROC) and surface crack density(SCD). L9 method used to design the experiment and GRA used to optimize the process.

2.7 **Objective**

In this subject of research the main machining parameters such as cutting speed, feed and depth of cut were considered to carry out the required experiment. The various objective associated with the research work are given below

I. To know how the cutting speeds, feed rate and depth of cut affect the machinability aspect such as cutting force, surface roughness and tool wear during the hard turning operation.
II. A study was made to investigate the impact of cutting speed and tool wears on white layer thickness.
III. Finally, the comparison of force is done between the results of Finite Element Model with the result of experimentally measured data.

Chapter 3

Materials and methods

3.1 Experimental details

3.1.1 Work piece material

AISI 4140 is also known as chromium molybdenum alloy steel as this low alloy steel contains chromium and molybdenum its strengthening agent. Chromium provides good hardness penetration whereas molybdenum maintains uniform hardness and high strength, throughout this alloy. This alloy steel appeared as overall combination of toughness, strength, abrasion, and high fatigue strength and wear resistance.

Figure 11 Work piece AISI 4140 alloy steel

Work piece (AISI 4140) is prepared at Kalunga Cast Profile Limited. The work piece has a length of 600mm and diameter of 50 mm was initially used for turning. Heat treatment process is applied to make it's hardness up to 55 HRC.

3.1.2 Chemical composition

Following Table 1 shows chemical composition of AISI 4140 alloy steel.

Table 1 Composition of AISI 4140 alloy steel

Material Grade	C	SI	Mn%	S%	P	Cr	Mo
AISI414	0.38-	0.15-	0.75-	0.040max	0.035ma	0.80-	0.15-0.25

3.1.3 Mechanical properties

Table 2 Mechanical properties of AISI 4140 grade alloy steel

Tensile strength (MPa)	Yield strength	Elastic modulus	Shear modulu	Rockwell Hardness
655	415	190-	80	92

3.1.4 Application

AISI 4140 is used extensively in most industrials sector due to its wide range of application such as tool bodies, connecting rods, crank shaft, bolts, axles, jigs and fixtures, rams, guides, hydraulic machinery parts.

3.2 3Description of cutting tool

During the machining of hard material, temperature and force induced is very high. Large amount of heat was generated due to the friction between tool and chip as well as tool and machined surface. Therefore for a smooth machining cutting tool insert should overcome these difficulties.

(a) Tool Designation

SNMG 12 04 04

S-Insert (square) shape

N-Angle of clearance(0)

M- Medium Tolerances

G - Insert Features

12- It stands for the length of each cutting edge i.e. 12mm

04- It stands for nominal thickness of insert i.e. 4mm

04 – It stands for nose radius i.e. 0.4mm

Figure 12 Cutting tool insert

(b) Geometry of insert

Inclination angle	- 6°
Orthogonal rake angle	6°
Orthogonal clearance angle	6°
Auxiliary cutting edge angle	15°
Principal cutting edge angle	75°
Nose radius	0.4mm

(c) Tool holder

The tool holder used in above experiment for machining AISI 4140 alloy steel is PSBNR1616.

Figure 13 Cutting tool holder

(d) Tool holder specification

P : Clamping method (hold via bore)

S : Inset shape (square)

B: Style (75^0)

N: Angle of clearance (0°)

R: Direction of cutting (right handed)

16: it indicates the height of the shank i.e. 16mm

16: it indicates the width of the shank i.e. 16mm

3.3 Scanning Electron Microscope (SEM)

A standard scanning electron microscope (SEM) generally used for low to medium magnification (10-50,000×) visualize conductive samples. For a nonconductive sample to eliminate the charging effect, a conductive coating of carbon, gold, chromium is performed. Variable pressure is also used for a polymer and biological material without applying conductive coating.

To visualize the “White layer” and study the microstructural arrangement of AISI 4140 after machining, a scanning electron microscopy Shown in Figure 14 (SEM-JEOL-JSM-6480 LV machine) was used.

Figure 14. Scanning electron microscope

3.4 Talysurf instrument

Talysurf (1984) was the principal instrument ever to measure texture, form and contour simultaneously. Roughness, waviness, and dimensions are the main quantitative elements of a surface. The (Taylor Hobson Surtronic 3+) shown in Figure 15 was used to measure surface roughness by calculating average or mean value.

Figure 15 Talysurf (Model Taylor Hobson Surtronic 3+

3.5 Optical Microscope

Optical microscopes are universally used to generate a magnified view or photographic image of a small object. The arrangement of visible light and a system of lenses magnify the small samples with in human visualization. The model shown in Figure 16 was used to measure the tool wear in present research.

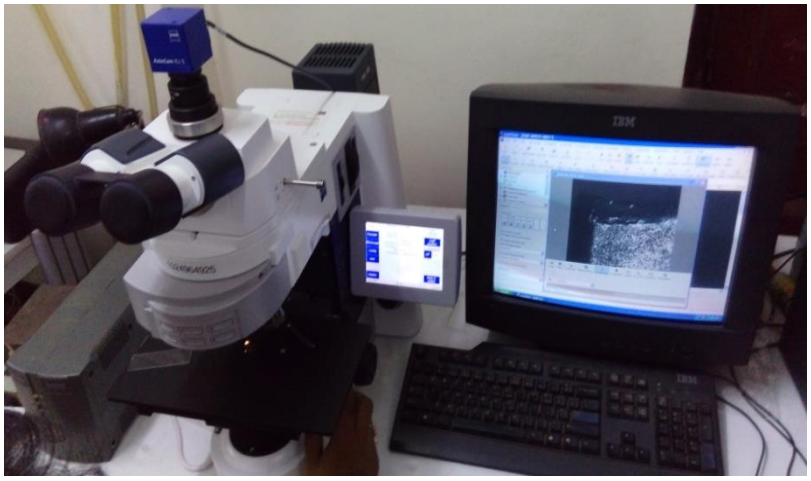

Figure 16 Optical Microscope

3.6 Wire- cut Electric Discharge Machining

The modification of EDM is generally established as wire-cut EDM, in which a thin metallic wire fed on to the work piece material. Shown in Figure 17

Figure 17 Wire-cut Electric Discharge Machining

The wire which is continually supplied from a spool immerse in a dielectric tank. It is guided between upper and lower guides made of by diamond. In this the work table should have moments in x and y-axis to cut the work piece material. It can able to cut a 300 mm thick plate with complex shape. In present work it is used to cut a 10*5 mm pieces from machined work piece to study the white layer.

3.7 Micro hardness tester

The essential guideline to measure micro hardness of a material is to observe the material resistant for plastic deformation, to know the hardness number a previously defined load is applied on the surface of a work piece material for a particular time. The impression formed due to the indentation is observed for calculating the hardness number. Shown in Figure 18.

Figure 18 Micro hardness tester

Chapter 4

Experimental details

The conventional lathe (HMT) machine was used to perform the hard turning operation of AISI 4140, Cr-Mo alloy steel. It maintains a high rigidity to counter act the vibration generated during hard turning. The process was carried out with different cutting parameters on dry condition. The PSBNR 1616 tool holder and SNMG 120404 Tic coated carbide inserts were used to fulfill the machining operation and the strain gauge dynamometer was used to measure the force obtained during hard turning. Every experimental run was carried out for 60 second and the chips were collected for future analysis.

Figure 19 Experimental setup

Table 3 Cutting control parameters with levels

Speed	150	430	710
Feed	0.1	0.13	0.15
Depth of cut	0.5	0.75	1

4.1 Experimental procedure

The objective of the experimental work was to find out the effect of two process parameters, cutting speed and flank wear on depth of the white layer. They were selected as cutting forces are insensitive to speed, most literature shows that flank wear is a critical variable for formation of white layer The experimental investigation also continue to determine the effect of speed, feed, depth of cut on output response such as force, surface roughness and tool wear and established a correlation between them. The experimental work was performed on a center lathe machine at Central Workshop of NIT Rourkela. The detail of the experimental set up was shown in Figure 19. The length and diameter of the work piece were taken as 600 mm and 50 mm respectively. The chemical composition and mechanical properties of the work piece are shown in Table 1 and 2. accordingly. The facing and centering action are performed on the work piece by carbide center drill. The work piece material hardness was measured as 58 HRC by micro hardness tester. Machining operation was performed on the work piece by using SNMG 120404 cutting insert. The levels of speed, feed, and depth of cut are shown in table 3. A three-factor three-level full factorial design was used to perform a total 27 no of experiments. Work piece turned for 1 minute for each set of data so 27 cuts were formed on the work piece shown in Figure 4. Force (Fz) value was measured by strain gauge dynamometer. The surface roughness (Ra) value was measured for 27 cuts by using Taylor/Hobson, Surtronic 3+ instrument and tool wear was measured by optical microscope. Again the work piece was machined with three different cutting velocity and keeping feed and depth of cut constant with three different flank wear. Three samples were cut from the work piece with the help of wire EDM. Then the samples were polished with four different grades of sand papers after that cloth and diamond polishing were performed. Then the samples etched with 2% nital (2ml HNO_3+98ml methanol) solution for 15 to 20 second. Microstructure for white layer was observed by scanning electron microscope.

The experiments were performed with three levels of cutting speed, feed rate and depth of cut and the output response such as force, surface roughness, tool wear given in Table 4.

Table 4 Experimental values for force (Fz), Surface roughness (Ra), and tool wear (tw)

Run Order	Speed (m/min)	Feed (mm/rev)	D.O.C (mm)	Force (F_z)N	S.R (μm)	Tw (mm)
1	23.56	0.10	0.50	101	2.04	0.842
2	23.56	0.10	0.75	169	1.74	0.660
3	23.56	0.10	1.00	140	1.80	0.675
4	23.56	0.13	0.50	93	2.70	0.552
5	23.56	0.13	0.75	210	2.00	0.961
6	23.56	0.13	1.00	182	2.10	0.860
7	23.56	0.15	0.50	104	2.66	0.782
8	23.56	0.15	0.75	260	2.22	1.062
9	23.56	0.15	1.00	160	2.04	0.893
10	67.54	0.10	0.50	81	1.72	0.911
11	67.54	0.10	0.75	115	2.34	0.962
12	67.54	0.10	1.00	160	2.98	0.781
13	67.54	0.13	0.50	94	1.30	1.670
14	67.54	0.13	0.75	160	2.00	0.820
15	67.54	0.13	1.00	195	2.30	1.431
16	67.54	0.15	0.50	99	2.08	0.540
17	67.54	0.15	0.75	180	2.22	0.440
18	67.54	0.15	1.00	190	2.30	1.130
19	111.52	0.10	0.50	112	2.00	1.112
20	111.52	0.10	0.75	170	2.30	1.761
21	111.52	0.10	1.00	150	2.00	1.434
22	111.52	0.13	0.50	98	2.10	0.261
23	111.52	0.13	0.75	120	1.90	1.201
24	111.52	0.13	1.00	190	1.77	0.601
25	111.52	0.15	0.50	116	1.96	0.873
26	111.52	0.15	0.75	180	1.58	0.440
27	111.52	0.15	1.00	165	1.85	0.890

Chapter 5

Results and Discussion

5.1 Analysis using full factorial design

In recent decade a continuous trend is going on to use appropriate design for performing the experiment. There are various methods used such as full factorial design, Taguchi, Response Surface Methodology to find out the optimal combination of process parameters [1] investigate to find out a mathematical model for cutting force, thrust force, cutting temperature and surface roughness. A 3^3 full factorial design was used for obtained a parametric analysis [9] studied to develop a cutting force model by considering a tool thermal property. The model predicts low major cutting force and low thrust force but high chip- tool interface temperature.

In present research a statistical model was introduced for performance characteristic (force, surface roughness, and tool wear) by using full factorial design.

5.1.1 Methodology

Full Factorial Design consists of all possible sequence of a set of factors. It is a full proof design approach in which an experimental run can be performed at every combination of factor level. A full factorial design of experiment provides most information about main effect factor and interaction factor. The process output linked to the input variable is known as Response. Controlled or Uncontrolled variable whose influence is studied is called factor and setting of factor (+, -, 1, -1 hi, lo, alpha, numeric) is called as level.

Analysis of variance (ANOVA) is a statistical method or technique used to determine the degree of inequality or affinity among a group of data. This method is established by comparing the average value of a common component. It provides a statistical test to know about the means of several groups that whether they are equal or not. A lot of fluctuation occurs in most experimental trials so it was a huge finding from

experimentation. There are some equations to calculate all the data in ANOVA table by manual method. The result of a factorial design may be extended to the general case. In which there are three levels and three factors arranged in a factorial experiment. In normal case if there will be (abc ⋯⋯ n) no of total observation 'n' no of replicates are there and all the factors in the experiments are fixed. Then the main effect and interaction can be easily developed. For a fixed effect model main effect and interactions can be easily formulated by dividing the corresponding mean square for the effect or interaction by mean square error. The number of degree of freedom for any main effect is the number of levels minus one, and no of degree of freedom for an interaction is the product of the number of degree of freedom associated with individual component of the interaction. Equation to determine ANOVA test value manually is given below.

The standard formula to find out total sums of squares shown in Equation 1.12

$$ss_T = \sum_{i=1}^{a}\sum_{i=1}^{b}\sum_{i=1}^{c} y_{i\ ijk}^2 - \frac{y^2}{abn} \tag{1.12}$$

The sum of square of main effect for A treatment (SS_A) shown in Equation 1.13

$$ss_A = \frac{1}{bn}\sum_{i=1}^{b} y_{i\ \ldots}^2 - \frac{y_{\ldots}^{\ 2}}{abn} \tag{1.13}$$

The sum of square of main effect for B treatment (SS_B) shown in Equation 1.14

$$ss_B = \frac{1}{an}\sum_{j=1}^{b} y_{j\ \ldots}^2 - \frac{y_{\ldots}^{\ 2}}{abn} \tag{1.14}$$

Sum of square due to sub totals shown in Equation 1.15

$$ss_{subtotal} = \frac{1}{n}\sum_{i=1}^{a}\sum_{j=1}^{b} y_{ij}^2 - \frac{y_{\ldots}^{\ 2}}{abn} \quad \ldots\ldots\ldots\ldots\ldots\ldots\ldots \tag{1.15}$$

Sum of square contain SS_A and SS_B shown in Equation 1.16

$$SS_{AB} = SS_{subtotals} - SS_A - SS_B \quad (1.16)$$

Sum of square for error can be calculated by subtraction shown in Equation 1.17

$$SS_E = SS_T - SS_{AB} - SS_A - SS_B \quad (1.17)$$

The high chromium steel (AISI 4140) was machined in the experimentation section. The process parameter, cutting condition and tooling were discussed in same section. The test showed some result on basic of Full Factorial Design.

5.1.2 Effect of process parameters on force (Fz)

By comparing the forces in ANOVA test the output is represented in Table 5. The main effect plot displayed in Figure 20 provides the information that at 430rpm, 0.1mm/rev and 0.5mm depth of cut force value obtained is minimized. The Tangential force (Fz) will increase with increase in depth of cut, feed rate and cutting velocity respectively. The depth of cut is the most influential parameter on cutting force.

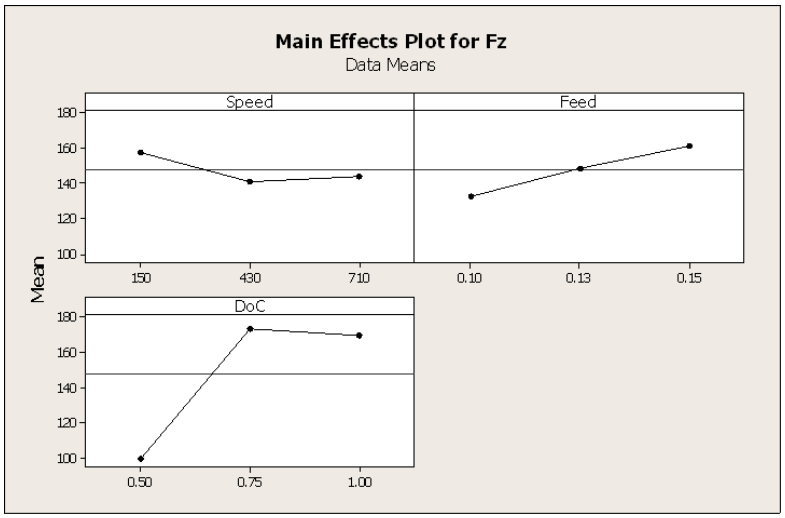

Figure 20 Main effect plot for Fz

From the ANOVA table it was concluded that doc followed by the interaction between speed and doc are most influential parameters for force (Fz) with percentage of contribution of 61.82, 13.34 respectively. The R- sq value for force is 95.63% which

indicates that prediction for response is very good in presented model. Run order plot, Fit value plot and normal probability plot are presented in Figure 21

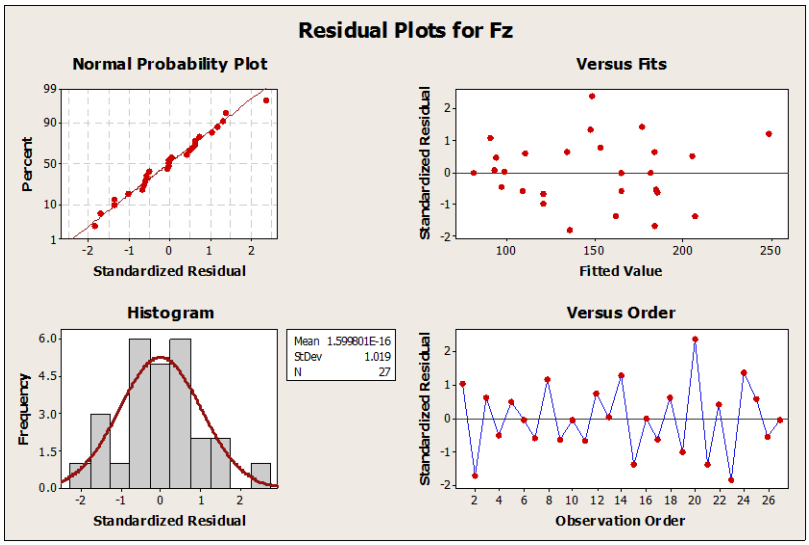

Figure 21 Residual plot for Fz

Table 5 ANOVA test for Force (Fz)

Source	DF	Seq SS	Adj SS	Adj MS	F	P	%contribution
Speed	2	1321.4	1321.4	660.7	2.39	0.154	0.00026
Feed	2	3659.9	3659.9	1829.9	6.61	0.020	7.21
Doc	2	31353.2	31353.2	15676.6	56.59	0.000	61.82
Speed*Feed	4	1471.9	1471.9	368.0	1.33	0.338	2.90
Speed*Doc	4	6767.9	6767.9	1692.0	6.11	0.015	13.34
Feed*Doc	4	3921.5	3921.5	980.4	3.54	0.060	7.73
Error	8	2216.1	2216.1	277.0			
Total	26	50711.9					
S=16.6436			R-Sq=95.63%			R-Sq (adj)=85.80%	

*significant influence (α=0.05)

Regression Equation**:** The mathematical model shown by equation 1.18 was developed to analyze the effect of force in terms of cutting parameters.

Fz = -13 + 0.119*speed + 499*feed + 53*doc – 1.09*speed*feed – 0.006 speed*doc + 712 feed*doc (1.18)

5.2 Effect of process parameters on surface roughness

Lower-the-better principle is maintained to visualize the effect of process parameter on Surface Roughness. The ANOVA test shows that interaction of speed, depth of cut and speed, feed were appeared as a significant process parameter for surface roughness with a contribution of 46.87% and 25.95% respectively, shown in Table 6. From main effect plot it was concluded that the Ideal condition to achieve a better surface roughness value is at a speed 0f 710rpm feed value of 0.15mm/rev and depth of cut of 1mm. As speed increases mean of surface roughness value decreases it indicates that good surface finish is obtained with increase in speed.

Table 6 ANOVA test for surface roughness (Ra**)**

Source	DF	Seq SS	Adj SS	Adj MS	F	P	% contribution
Speed	2	0.24287	0.24287	0.12144	3.14	0.099	7.61
Feed	2	0.04112	0.04112	0.02056	0.53	0.607	1.28
doc	2	0.04110	0.04110	0.02055	0.53	0.608	1.28
Speed*feed	4	0.82766	0.82766	0.20691	5.34	0.022	25.95
Speed*doc	4	1.49508	1.49508	0.37377	9.65	0.004	46.87
Feed*doc	4	0.23157	0.23157	0.05789	1.49	0.291	7.26
error	8	0.30985	0.30985	0.03873			
Total	26	3.18925					
S= 0.196803			R-Sq = 90.28%			R-Sq (adj) = 68.42%	

*Significant influence (α=0.05)

Surface roughness value increases with increase in feed. Mechanical vibration is also recognizing as an effect which influence surface roughness. Interaction effect of feed is more influencing than individual effect. Surface roughness increases with increases in depth of cut up to 0.75mm. Better surface finish is achieved at a depth of cut of 1mm. The R-sq value above 90% indicates that predicted model can be accepted in this present design.

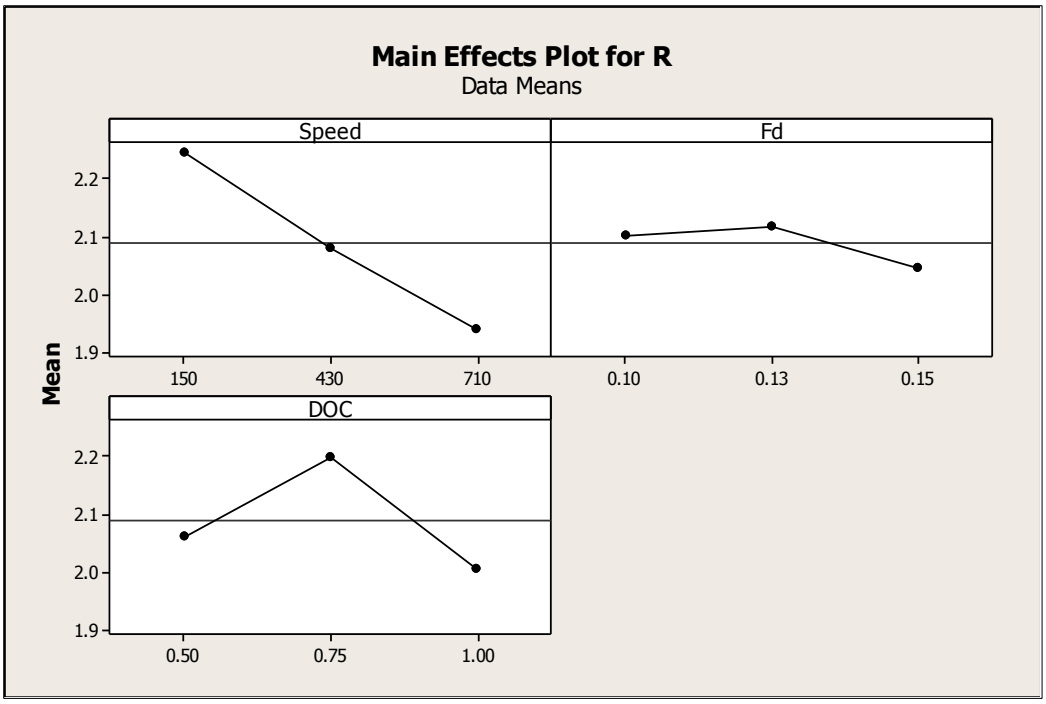

Figure 22 Main Effects plot for surface roughness

The regression equation modeled for Ra is shown in equation 1.19

R = -0.88 + 0.00220*speed + 26.9*feed + 2.20*doc – 0.0274 speed*feed + 0.00121 speed*doc – 20.5 feed*doc (1.19)

From the normal probability plot it was observed that the residual percentage for each run is closed to standard residual line. Residual vs observation data shows that the values are commonly scattered, so variables are significantly affecting the Surface roughness value. Run order plot for each Ra is shown in Figure 23

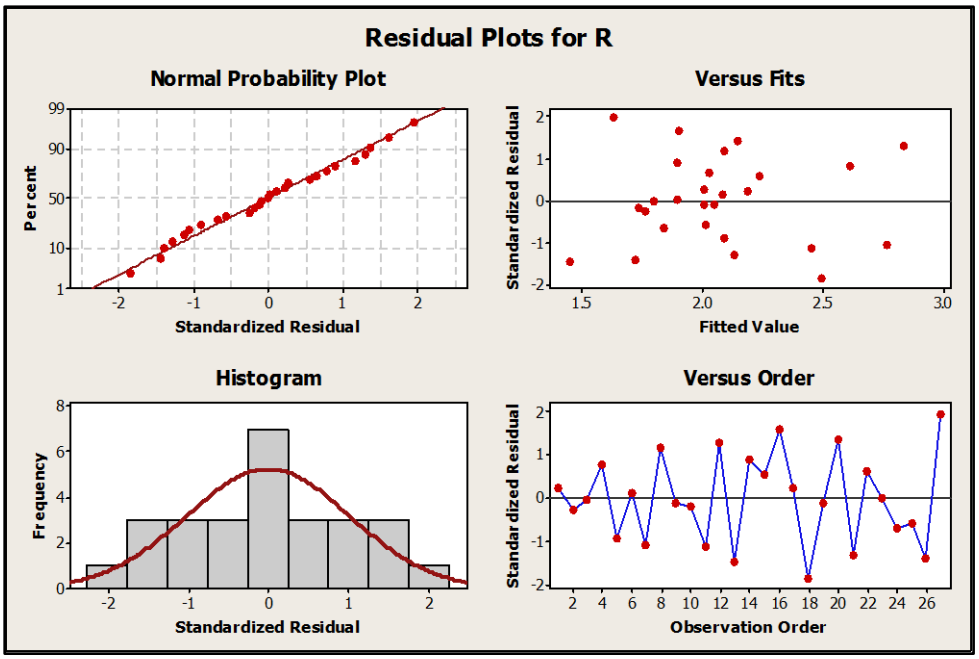

Figure 23 Residual plots for Ra

5.3 Effect of process parameters on tool wear (tw)

Tool wear was estimated by using Optical Microscope shown in Figure (16). ANOVA trial for tool wear explains that cutting speed is the most influencing factor for tool wear. The main effect plot for tool wear shown in Figure 24. The percentage of contribution of the process parameters and their interaction for tool wear are shown in in table 7. The interaction between speed and feed is considered as most efficient parameters affecting tool wear. Present investigation shows that tool wear increases with increase in cutting speed followed by feed rate and depth of cut respectively. The maximum tool wear value found out at 430rpm, 0.15mm/rev and 0.75mm depth of cut.

Table 7 ANOVA test for tool wear (tw)

Source	DF	Seq SS	Adj SS	Adj MS	F-Value	p-Value	%contribution
speed	2	0.2153	0.2153	0.10763	4.2	0.057	7.71
feed	2	0.1937	0.1937	0.09687	3.78	0.07	7.07
doc	2	0.2081	0.2081	0.10403	4.06	0.061	7.47
Speed*feed	4	1.2006	1.2006	0.30014	11.7	0.002	43.02
Speed*doc	4	0.5574	0.5574	0.13934	5.43	0.021	19.97
Feed*doc	4	0.2101	0.2101	0.05252	2.05	0.18	7.52
Error	8	0.2052	0.0257				
Total	26	2.7903					
S = 0.1601		R-Sq=92.65%			R-sq (adj) =76.10%		

Regression Equation**:** The second order equation for tool wear is shown in equation 1.9

Tw = 0.32 – 0.00164*speed + 7.6*feed + 0.64*doc + 0.0106 speed*doc + 0.00016 speed*doc – 9.5 feed*doc (1.20)

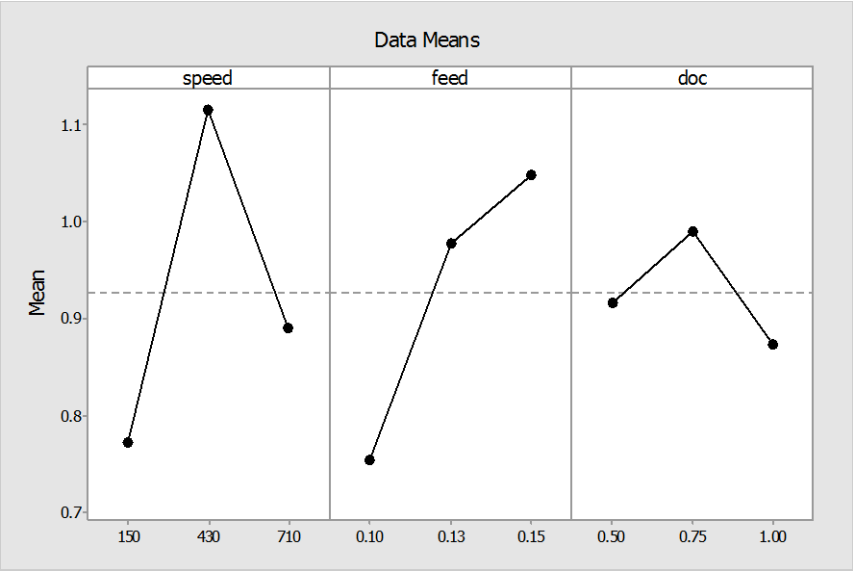

Figure 24 Main effect plots for tw

Residual plots for tool wear are presented in figure 25. It is used to figure out the data for analysis and regulate the data to show that whether the model fits the data for the assumption analysis. The data point closed to the straight line indicates the consistency of data obtained from experimentation. Commonly scattered data indicates that tool wear is significantly affected by variables.

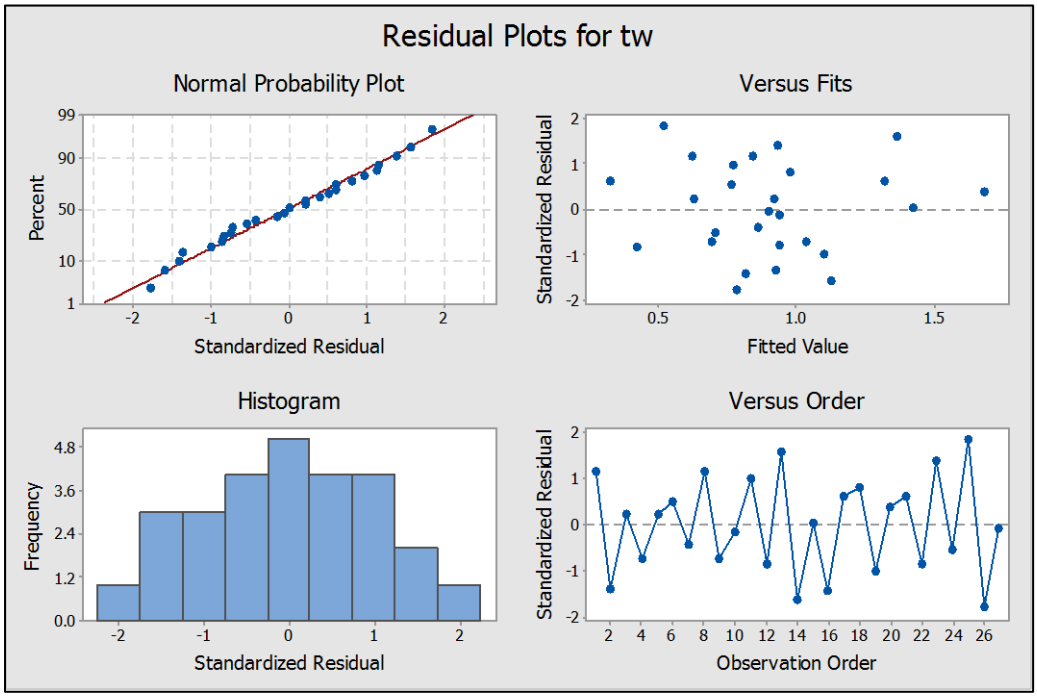

Figure 25 Residual plots for tw

The optimum setting of parameters as per full factorial design for minimum tool wear, minimum surface roughness, and minimum force were concluded from above results. The optimum conditions are given below

- For force: 430rpm, 0.1 mm/rev, and 0.5mm depth of cut.
- For surface roughness 710rpm, 0.15 mm/rev and 1mm depth of cut.
- For tool wear 150rpm, 0.1 mm/rev and 1mm depth of cut.

5.4 GRA based multi-response optimization

5.4.1 Introduction

Formerly, for designing experiments researchers are frequently use single response optimization such as Taguchi method, Factorial design, and Response surface methodology, as it able to optimize only one objective function at a time so to optimize multi objective function, in modern days authors have more focused on multi-response optimization technique such as Grey Relation Analysis, Regression Analysis Method, Artificial Neural Network etc. The Grey Relation Analysis (GRA) was implemented to find out a solution for a system, where the data is deficient or the model is uncertain.[15] In addition it also provides solution to the multi input and distinct data problem. In Grey relation analysis (GRA) white demonstrate full information about the data where as black represent nil information about data and grey speaks to inadequate data. In this paper, A single response optimization method (Full factorial) is used to find out the optimum condition for force (Fz), surface roughness (Ra), tool wear (tw) by machining AISI 4140 alloy steel. From the investigation of single response like force, surface roughness and tool wear, the optimum cutting condition for different output responses are different. Therefore, to find an optimum condition for all output responses, a multi objective optimization is required. In present work the optimum cutting condition has been found out by Grey relation analysis method.

5.4.2 Optimization Procedure

Grey Relation Analysis deals with the incomplete and inaccurate experimental data very efficiently and statistically. The experimental data were normalized between zero to one to avoid the problem of distinct scales and unit. “Lower the better” performance characteristic is applied for force (Fz), surface roughness (Ra) and tool wears (tw). The procedures involved in GRA are

In the first step responses are normalized by using equation (1.21) shown in Table8. The quality loss estimated for each individual has been calculated and listed in Table 9. Then the overall gray relation condition and respective gray relation condition have been calculated by using equation (1.24). The distinguishing coefficient value always assumed between 0 and 1, here it is assumed to be 0.5. The overall grey relation condition exhibit

the quality index of multiple response of process. Thus the multi objective optimization is converted to single objective optimization.

There are three different types when normalization depends upon the target of response. It also provide a comparable sequence of Lower is better (LB), Higher is better (HB), and nominal is better (NB).

$$X_{ij} = \frac{Y_i(K) - \min Y_i(k)}{\max Y_i(K) - \min Y_I(K)} \tag{1.21}$$

Where, the equation (1.21) used to normalize "higher-the-better" performance characteristic

$$X_{ij} = \frac{\max Y_i(K) - Y_i(k)}{\max Y_i(K) - \min Y_I(K)} \tag{1.22}$$

Above equation (1.22) characterize for lower-the-better performance characteristic

$$X_{ij} = 1 - \frac{\left[Y_I - Y_{0b}(k)\right]}{\max Y_i(K) - \min Y_{0b}(K)} \tag{1.23}$$

Above equation (1.23) used for "nominal-the-better" performance characteristics.

Normalized value for run of K^{th} responses is represented by X_i (k). min Y_i (k) shows the smallest value of Y_i (k) for K^{th} response and max Y_i(k) is the largest value of Y_i(k) for k^{th} response and x is represented as a normalized array.

Grey relation co-efficient (γ) can be evaluated by the equation (1.24) as follows

$$\gamma_{il} = \frac{\Delta_{\min} + \xi\Delta_{\max}}{\Delta_{0,i}(k) + \xi\Delta_{\max}} \tag{1.24}$$

Where $\Delta_{0,I}$ (k) represent the deviation sequence and it is calculated by the difference between $X_0^*(k)$ and $X^*_i(k)$. Distinguishing coefficient is termed as ξ and its value lies between 0 and 1. ξ is taken as 0.5 for this study. Δ_{max} and Δ_{min} are maximum and minimum value of deviation.

5.4.3 Result and discussion:

The results obtained from the algorithm of Grey relation analysis after normalizing the variables are given in Table-8.

Table 8 Normalized value of process parameters for each performance characteristics

	Normalized value		
SL NO	X_{ij} (F)	X_{ij} (Ra)	X_{ij}(tw)
1	0.888268	0.559524	1
2	0.50838	0.738095	0.87069
3	0.670391	0.702381	0.857759
4	0.932961	0.166667	0.963793
5	0.27933	0.583333	0.611207
6	0.435754	0.52381	0.698276
7	0.871508	0.190476	0.765517
8	0	0.452381	0.524138
9	0.558659	0.559524	0.669828
10	1	0.75	0.65431
11	0.810056	0.380952	0.75
12	0.558659	0	0.766379
13	0.927374	1	0
14	0.558659	0.583333	0.732759
15	0.363128	0.404762	0.206034
16	0.899441	0.535714	0.060345
17	0.446927	0.452381	0.663793
18	0.391061	0.404762	0.465517
19	0.826816	0.583333	0.87931
20	0.502793	0.404762	0.405172

21	0.614525	0.583333	0.922414
22	0.905028	0.52381	0.836207
23	0.782123	0.642857	0.40431
24	0.391061	0.720238	0.921552
25	0.804469	0.607143	0.687069
26	0.446927	0.833333	0.318966
27	0.530726	0.672619	0.672414

5.4.4 Grey relation grade (GRG)

Grey Relation Grade (GRG) analyzed the performance of various characteristic. As a rule, higher is better. GRG show better multiple performances characteristic and corresponding parameter is thought to be near to the ideally normalized value. GRG is represented as the average of all GRC value. For all experimental run GRG values are calculated and it is observed that for highest GRG value process parameter is considered to be better than any other. The optimal parametric combination evaluated by maximizing over all Grey Relation Grade (GRG). The highest GRG value is 0.78299 and the corresponding process parameters for this value are 23.56m/min speed, 0.1mm/rev feed, 0.5mm doc.

Table 9 generation of GRC with GRG

Grey relation co efficient and grade				
SL NO	GRC (F)	GRC (Ra)	GRC (tw)	GRG
1	0.817352	0.531646	1	**0.782999**
2	0.504225	0.65625	0.794521	0.651665
3	0.602694	0.626866	0.778523	0.669361
4	0.881773	0.375	0.932476	0.72975
5	0.409611	0.545455	0.562561	0.505875
6	0.469816	0.512195	0.623656	0.535222
7	0.795556	0.381818	0.680751	0.619375
8	0.333333	0.477273	0.512367	0.440991
9	0.531157	0.531646	0.602285	0.555029
10	1	0.666667	0.591233	0.752633
11	0.724696	0.446809	0.666667	0.612724

12	0.531157	0.333333	0.681551	0.515347
13	0.873171	1	0.333333	0.735501
14	0.531157	0.545455	0.651685	0.576099
15	0.439803	0.456522	0.386409	0.427578
16	0.832558	0.518519	0.347305	0.566127
17	0.474801	0.477273	0.597938	0.516671
18	0.450882	0.456522	0.483333	0.463579
19	0.742739	0.545455	0.805556	0.697916
20	0.501401	0.456522	0.456693	0.471538
21	0.564669	0.545455	0.865672	0.658598
22	0.840376	0.512195	0.753247	0.701939
23	0.696498	0.583333	0.456334	0.578722
24	0.450882	0.641221	0.864382	0.652162
25	0.718876	0.56	0.615058	0.631311
26	0.474801	0.75	0.423358	0.549386
27	0.51585	0.604317	0.604167	0.574778

5.4.5 Analysis of Variance

The GRG value obtained from Table.9 is taken as input factor for future investigation. Analysis of Variance used to determine that which process parameters have real impact on performance characteristic. Percentage of contribution of each process parameters towards the response also be found out by ANOVA table. Percentage of contribution was calculated by following expression

$$\%contribution = \frac{Sum \text{ of square of variation}}{Total \text{ sum of square of variaton}}$$

From ANOVA table it was concluded that depth of cut has maximum effect followed by feed and interaction between speed and depth of cut. The R^2 value greater than 90% indicates that predicted model can be accepted for present design.

Table 10 ANOVA test for GRG

source	DF	Adj SS	Adj MS	F- value	p- Value	% contribution
speed	2	0.008453	0.004226	2..21	0.172	3.35
feed	2	0.045003	0.022502	11.78	0.004	17.87
doc	2	0.115093	0.057546	30.13	0	45.71
Speed*feed	4	0.020619	0.005155	2.70	0.108	8.18
Speed*doc	4	0.037042	0.009260	4.85	0.028	14.71
Feed*doc	4	0.010281	0.002570	1.35	0.333	4.08
Error	8	0.015279	0.001910			
Total	26	0.251769				
S= 0.0437016			R-sq= 93.93%		R-sq ((adj)=80.28%)	

Regression Equation **T**he second order equation was developed to analyze the GRG value.

GRG = 1.587 – 0.000862*speed – 5.52*feed – 0.599*doc + 0.00525 speed*feed + 0.000270 speed*doc + 1.76 feed*doc (1.25)

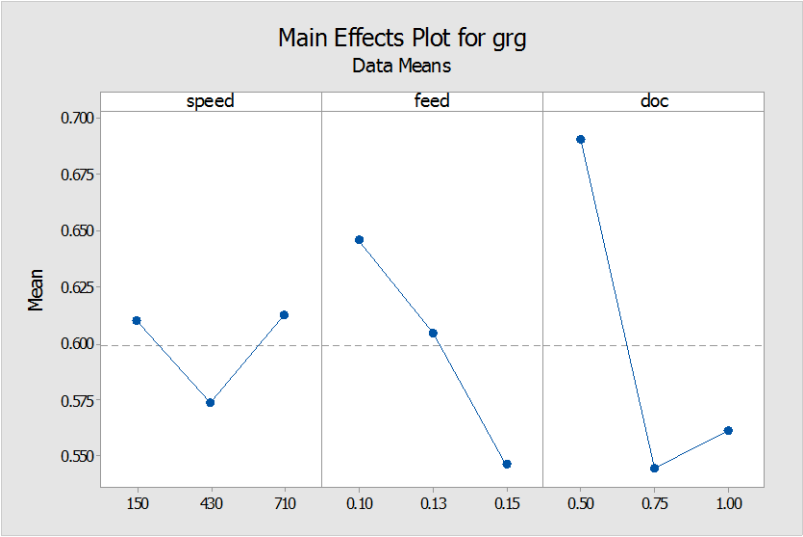

Figure 26 Main effect plot for GRG

The main effect plot exhibit the mean of weighted Grey Relation Grade determined by using Larger-the-better principle. The steep slope of Main effect plot graph shows the impact of machining parameters in their performance characteristic. The horizontal dotted line in the graph shows the overall mean of Weighted Gray Relation Grade. The optimum parametric condition for speed (150rpm), feed rate (0.10mm/rev), and depth of cut (0.5mm) was determined from main effect plot. Residual vs observation graph shows that data are commonly scattered and variables have significant effect on responses.

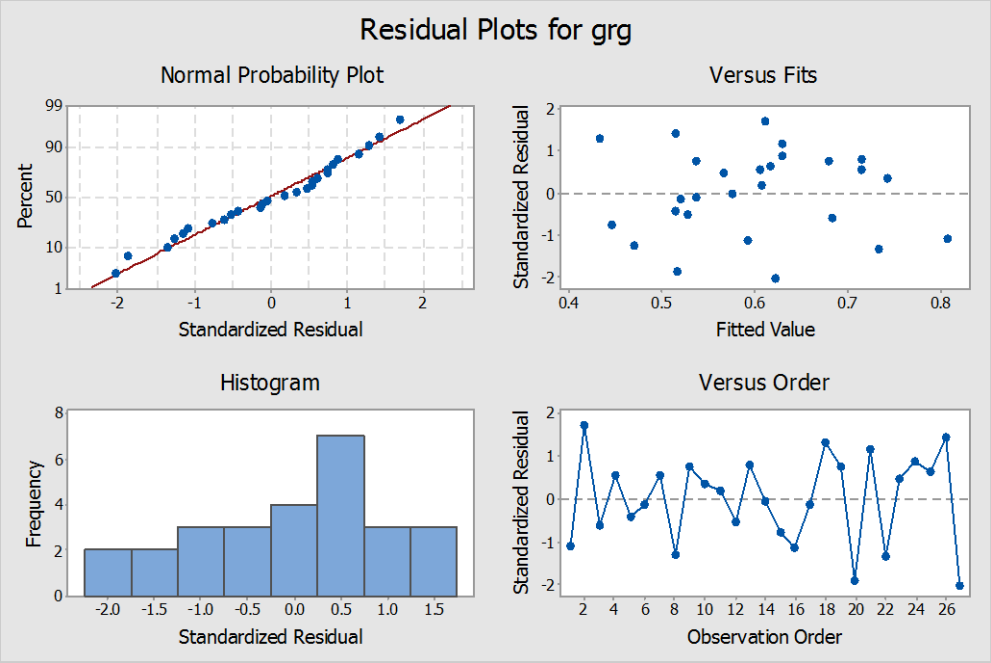

Figure 27 Residual plots for GRG

5.4.6 Conclusion:

In this study multiple performance characteristics on a hard turning operation was optimized by using Grey Relation Analysis and end of with below results

1. The depth of cut is considered as the most significant factor which influences the performance characteristics with 45.71% contribution.
2. The optimum process parameters obtained from GRA are 150rpm speed, 0.1mm/rev feed rates and 0.5 mm depth of cut.

5.5 Tool wear

The experiments were performed for all 27 run and corresponding chips were collected to study the behavior of the chips. The AISI 4140 alloy steel was machined to figure out the macro morphology of the chips by optical microscope. The chips were collected at different cutting speed, feed rate and depth of cut shown in Figure 28. The model of the acquired chip under this machining condition is continuous, snarled type and spiral type. It might be cause an issue for operator In the continuous and snarled type of chips. These types of chips are mainly obtained due to low depth of cut.

At an initial stage of turning a high value of chip thickness was observed in every machining condition. The high frictional force and tool wear are the principal cause to produce the light golden color chips, because the huge amount of heat produced at chip tool interface at the time of hard turning is carried away by chips. Feed rate has the potential to disturb the surface roughness as feed force increases wear of the tool increases leads to get poor surface finish.

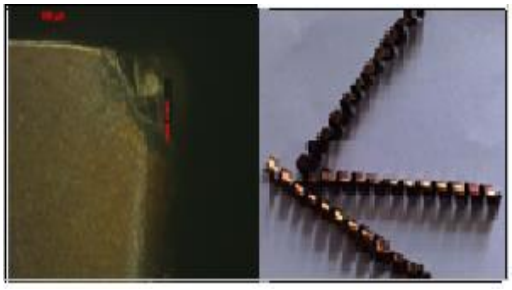

(1)

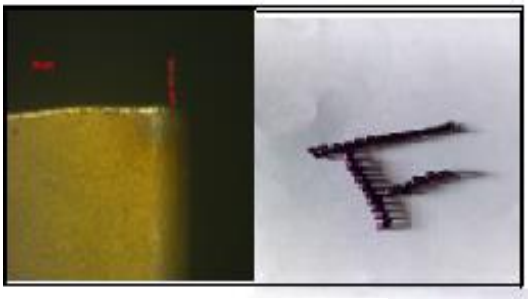

(2)

(3)

(4)

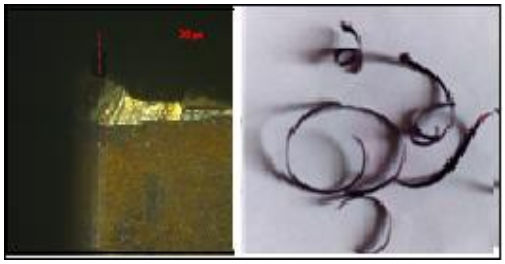

(5)

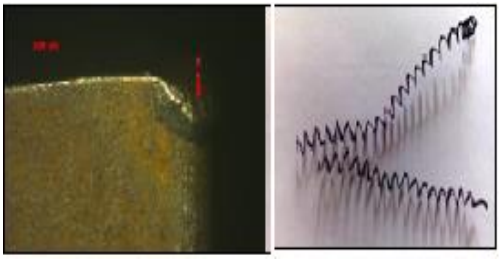

(6)

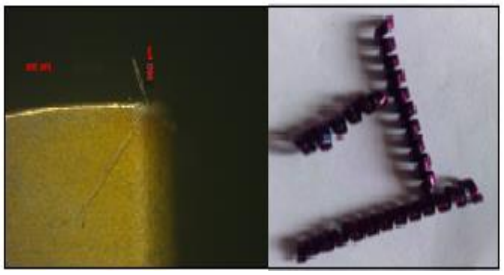

(7)

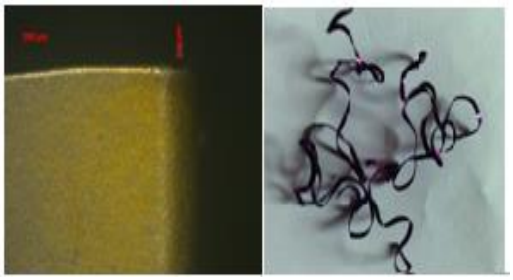

(8)

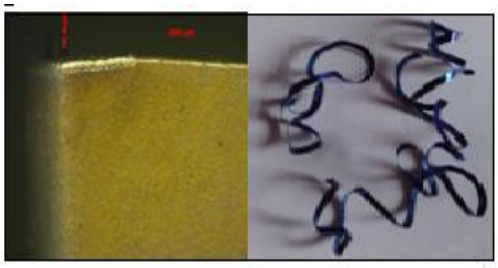

(9)

(10)

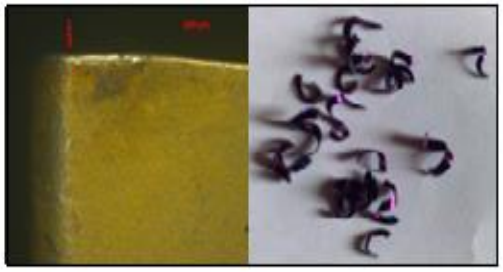

(11)

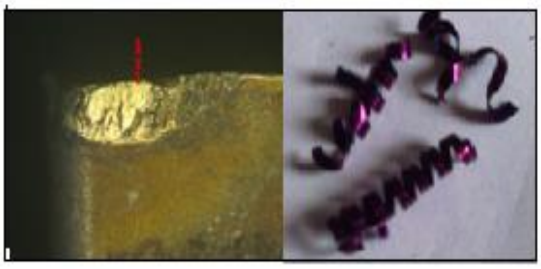

(12)

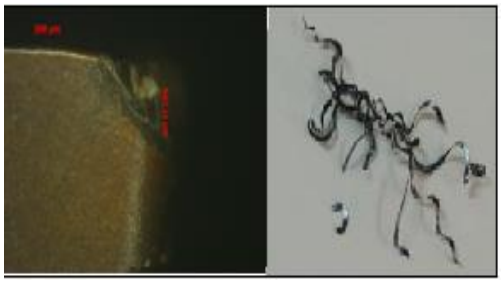

(13)

(14)

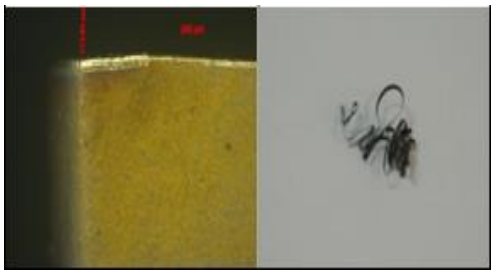

(15)

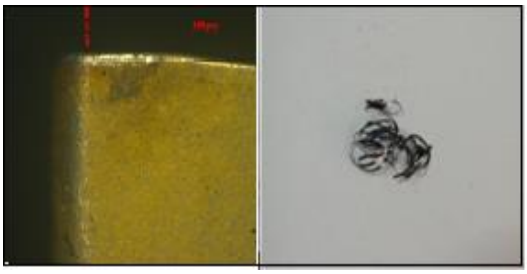

(16)

(17)

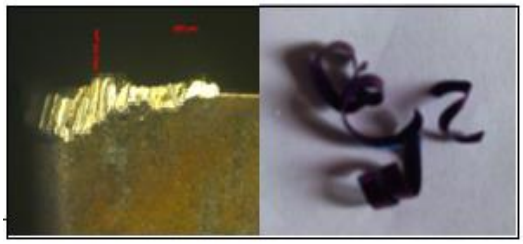

(18)

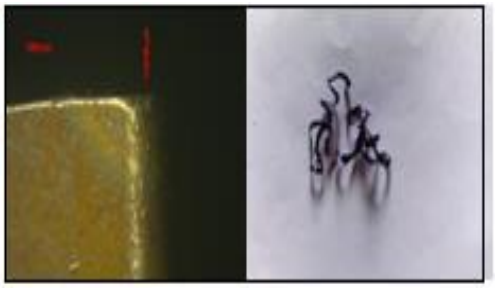

(19)

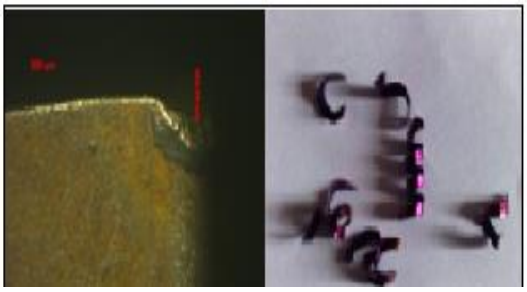

(20)

Figure 28 Tool wear and chip corresponding to the experiment number 1-20

5.6 White layer

Many researchers analyzed that temperature is the most influential parameter for generation of white layer on a hard turned component. As flank wear and cutting speed are extensively affect the cutting temperature, a study was made to investigate the impact of cutting speed and tool wears on white layer thickness. Experiments were performed at three different cutting conditions for three different wear values to find out the effect of cutting speed and tool wear on white layer thickness.

Hard turning was performed at low (23.5 m/min) moderate (65.5m/min) and high (111.5m/min) cutting speeds on AISI 4140 alloy steel with their respective tool wear combination. The observation was analyzed to experience the behavior of cutting speed and tool flank wear on white layer thickness

5.5.1 Effect of cutting speed

Cutting speed is considered as the most compelling parameter to generate work piece temperature so cutting speed should not be ignored during the study of white layer. The impact of cutting speed on thickness of white layer is presented in Figure 29. As cutting speed increases white layer thickness increase, and a slight reduction occur after achieving the highest value at around 250m/min, however in case of hard turning when cutting speed increases, temperature generation becomes high, but maximum amount of heat is taken away by the chips. So, work piece surface temperature decreases, so although heat increases the thickness of white layer decreases at high speed range.

5.5.2 Effect of flank wear

Flank wear is termed as a maximum influential parameter to generate white layer. It is observed in many studies that white layer thickness increases with increase in flank wear shown in figure 29. During machining, the rubbing action between flank and machined surface causes a stress and deformation in subsurface, which also reduce the transition temperature. Meanwhile, the heat in contact area between tool and machined surface accumulates with increase of flank wear. The graph between flank wear vs. white layer shown in Figure 29 (d).shows that as flank wear increases white layer thickness increases.

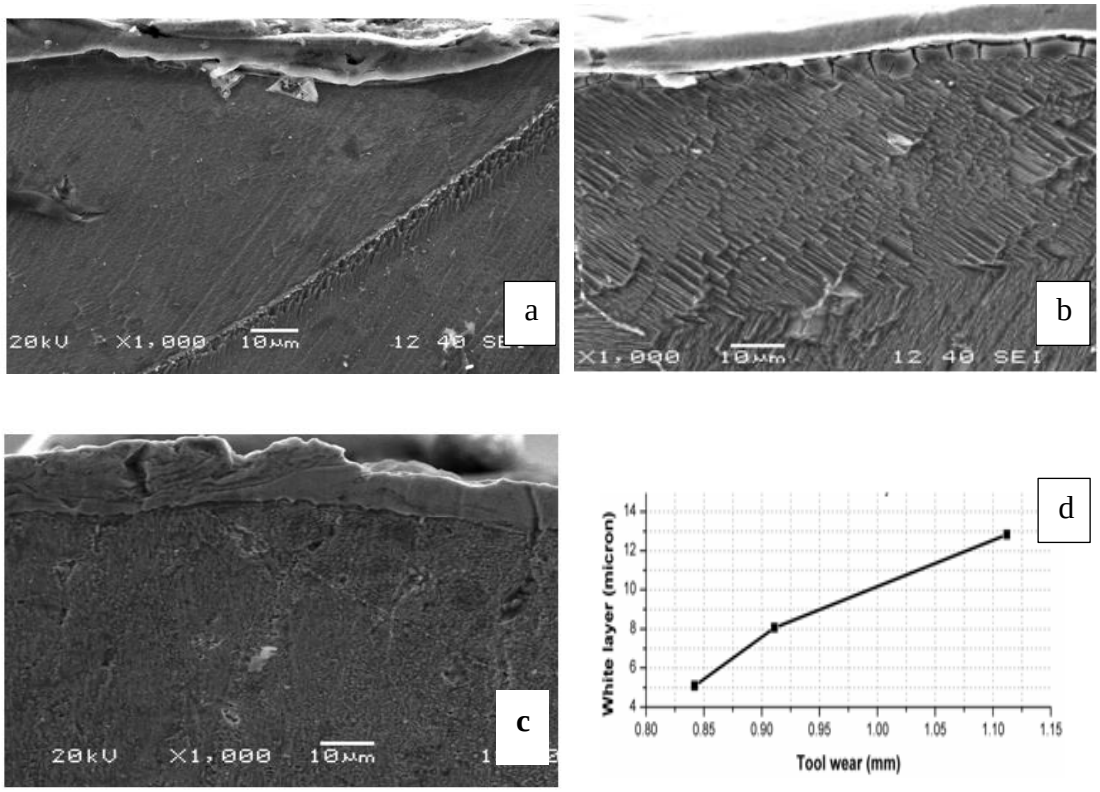

Figure 29 (a) Tw=0.842mm, wl thickness=5.098micron, (b) Tw= 0.911 wl thickness 8.067micron, and (c) Tw = 1.112 wl thickness = 12.831micron

5.5.3 Effect of depth of cut

The depth of cut likewise changed the thickness of white layer. Temperature and stress in a machined surface mostly influenced by cutting depth. Because, with increase in depth of cut contact area between tool and work piece increases so temperature will increases so thickness of white layer increases with increase in depth of cut.

Chapter 6

Finite Element Method (FEM)

6.1 Prediction of force using Finite Element Analysis

Generally, in machining process unwanted material is removed from a block of metal to get a desired product. Study of the material removal process such as turning and facing from its dynamic point of view is much important as the unusual changes occur during that process. In orthogonal turning basically two types of cutting forces comes into action i.e. axial and tangential. Tendency to measure these forces encountered various types of problems such as to adopt a reasonable technique to measure and analyze the cutting force component, error and uncertainty associated with the measuring instrument. Repetition in experiment is required to maintain the accuracy, but it increases the overall cost of the process. Finite Element Method is the only solution developed by the researcher to overcome this problem. In machining process FEM is used to measure the temperature at tool chip interface and work piece, measure the cutting forces and chip formation[10]. FEM is universally used to analyze stress developed in complicated air frame structure, automotive industry.

The primary concept of a Finite Elements Analysis (FEA) was developed from a special analysis i.e. a work which is going through the analysis was divided into a large number of small elements and the action is developed on this element to find out the result[30]. In order to reduce the cost in metal cutting process, Finite Element Method is considered as a primary tool for modeling and simulation. In machining most of the researcher use Finite Element method to describes the chip formation process in turning with the simulation result, stresses developed during machining process, tool wear and force. A number of software like MSC- Marc, Abaqus, DEFORM 2D/3D, AdvantEdge and ANSYS were developed for simulation of cutting process. Here the analytical model “DEFORM 2D” is used to predict the tangential force (Fz) generated during Hard turning of AISI 4140 steel. The finite element simulation software was established on process simulation systems

which incorporate the function for modeling, heat conducting, forming etc. DEFORM 2D possess some very good features like good robustness, powerful simulation engine and easy to use.

6.2 Description of Finite Element Method

Finite element method (FEM) is a numerical technique to solve differential and integral equation. A number of physical problems can be solved by Finite Element Method. This method basically comprises of accepting the piecewise continuous function for the solution and getting the parameter of the function in the way that decrease the error in solution. Furthermore, for several years, researchers have been using this method to predict the challenging outputs and processes which cannot be measured using experimental methods. Therefore, to implement the numerical methods to the industries, enhancing the productivity of the industries, this method is used to model and solve the physical problems.

In the present work, the hard turning is modelled using finite element method with the help of a commercial package, Deform 2D ^{TM}, to explore the effects of process parameters on the output responses like force, temperature, tool wear, interface temperature, chip morphology; the model has been prepared and validated. Unlike Deform 3D, the 2D model don't require more space in the system to simulate the physical problem despite of certain assumptions. The model is plastic- rigid type since the workpiece hardness is almost 55HRC whereas the cutting tool hardness is relatively higher than the workpiece. Therefore, deformation is prominent to the workpiece only and considered as plastic body and the tool is considered as rigid body.

A thermo-mechanical model has been developed using Deform 2D considering both physical and thermal properties of both the work piece and the cutting tool. The complete model can be classified into 3 major steps, such as

1. Pre- processor- The information of material and its condition are given as the inputs into pre- processor. The various input parameters are cutting speed, feed, and depth of cut along with the thermal properties like convection coefficient, heat

transfer coefficient, thermal conductivity and heat capacity for both the workpiece and cutting tool. It also includes processes such as

a. Geometry definition,
b. Material assignment,
c. Mesh generation,
d. Fracture criteria and re-meshing criteria
e. Temperature assignment
f. Material flow stress behavior using Johnson-cook model or power law etc..

2. Simulation- It is used to execute simulation according to the data fed in pre-processor for numerical calculation. The calculation is based on several types of complex and numerical algorithms such as, Lagrangian type, Euler type, advanced Lagrangian- Euler type etc. There are several iteration methods used to solve the physical problem packaged in Deform 2D like direct iteration, newton-Raphson method etc..
3. Post- processor- After the completion of simulation, post- processor is used to visualize and analyze the simulation data. Basically it is used to study the database files against the simulation engine and represent the results in graphical and visual pattern. The output responses like force, cutting temperature, tool wear, stress generation and effective strain can be extracted and predicted from the post processor.

6.3 Material models/design and methodology

To prepare the model, the optimum cutting velocity, feed and depth of cut obtained from the experimental investigation was used. The simulation was made using Deform 2D taking workpiece as plastic and tool as rigid material. The solution method used was based on the Lagrangian type. The work piece dimension was 3mm X 0.7mm with AISI 4140 as the material. The workpiece is discretized into 1668 no’s of tetrahedral elements with finer mesh at the tool and workpiece zone as depicted in the Figure 30.

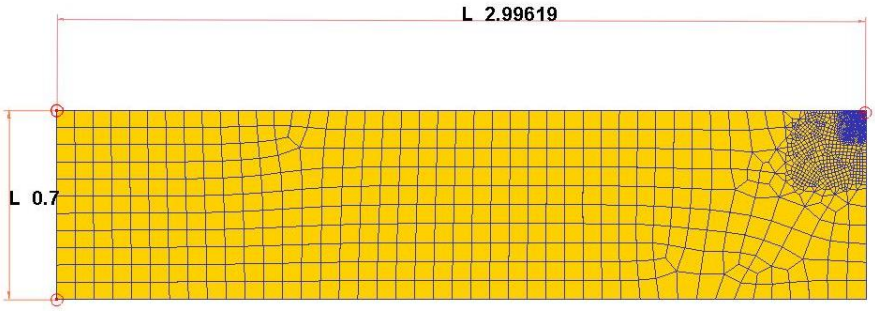

Figure 30 Meshed workpiece with the dimension

The cutting tool was discretized into 1174 no's of rigid type elements. The reason for the finer mesh is to run a smooth simulation and to get an accurate solution. The initial temperature was 20^0C assigned to the workpiece. The flow stress model was a non-linear model, Johnson- Cook model expressed in the Equation 1.26

$$\sigma = (A + B\varepsilon^n)[1 + C\ln(\frac{\dot{\varepsilon}}{\dot{\varepsilon_0}})]\ [1-(\frac{T-T_{room}}{T_{melt}-T_{room}})^{\mathrm{m}} \quad (1.26)$$

Where, $\sigma\ is$ the material flow stress,ε is the plastic strain, $\dot{\varepsilon}$ is the strain rate. $\dot{\epsilon_o}$ is the reference strain rate, T is the material temperature, $T_{melt}$is the material melting point temperature and T_{room} is the room temperature. A is known as the yield stress, B is known as pre- exponential factor, C is the strain rate factor, n is the work hardening exponent and m is known as the thermal- softening exponent. The material constants are taken from literature reviews can be summarized in Table 11.

Table 11 Johnson- Cook model constants

Constants	A (MPa)	B(MPa)	C	m	n	
Value	595	580	0.023	1.03	0.133	

6.4 Kinetic boundary conditions

The kinetic boundary conditions were applied to the workpiece as shown in the Fig. 31. In the following the bottom surface was assigned with the cutting velocity of 23.5 m/min,

whereas, the side surfaces were kept with zero velocity. The top and cutting surface contact with the cutting tool was kept free to formulate the chip generation.

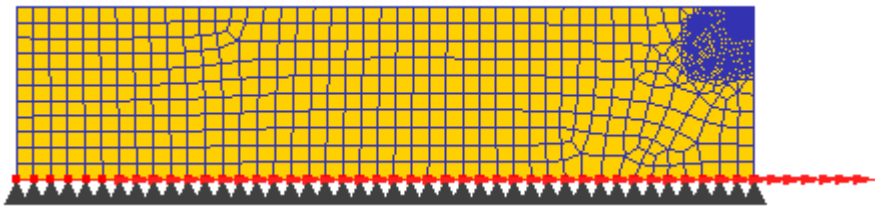

Figure 31 Kinetic boundary condition

6.5 Thermal boundary conditions.

To predict the thermal characteristics in the turning operation, the thermal boundary conditions were applied. The most influential factor affecting the temperature evolution in cutting tool and interface zone is the heat transfer coefficient, h. The boundary condition were defines as shown in the equation 1.27.

$$q = h(T_w - T_t) \qquad (1.27)$$

Where, q is the heat flux generated, T_w is the workpiece temperature and T_t is the tool temperature and h=10000 $W/m^2\ ^0C$ is the heat transfer coefficient. The side and top surfaces of the workpiece (Fig. 31) were assigned at room temperature allowing the heat transfer due to convection method to the environment. The heat transfer coefficient is responsible and the controlling factor for the heat propagation from the workpiece to the tool rake face. The convection coefficient that is responsible for the heat loss to the environment from the workpiece was assigned with a value of 0.4 $W/m^{2\ 0}C$.

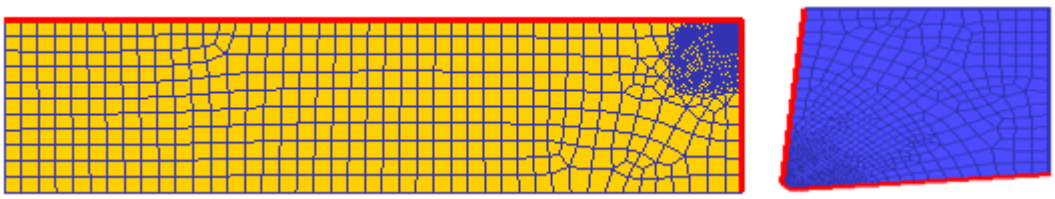

Figure 32 Thermal boundary condition applied

6.6 Tool Signature

The tool shape is described in a particular sequence called Tool signature. In this paper SNMG120404 cutting inserts were used for machining. Tool signature was stated in following according to Orthogonal Rake System (ORS)

$$\lambda - \Upsilon_0 - \phi_e - \phi - \alpha - \alpha_0 - r$$

Table 12 Signature of Cutting insert

λ	Inclination angle	6^0
Υ_0	Orthogonal rake angle	6^0
ϕ_e	End clearance angle	6^0
ϕ	Side clearance angle	6^0
α	Auxiliary cutting edge angle	15^0
α_0	Principal cutting edge angle	75^0
r	Nose radius	0.4mm

PSBNR 1616 has been used in machining operation.

Side cutting edge angle = -6^0, Back rake angle = -6^0, Side rake angle = -6^0

6.7 Boundary condition

1. For steady cutting operation the movement of the work piece was constrained from all (X, Y, Z) direction.
2. The cutting tool movement was in +ve Y direction and the location of cutting tool according to the work piece were shown in Figure 32.

Table 13 Thermal and mechanical properties of work piece material

Properties	Work Piece	Units
Thermal conductivity	42	$W\ m^{-1}\ K^{-1}$
Thermal Expansion	13.7	$\mu m\ m^{-1}\ K^{-1}$
Specific heat capacity		$J\ kg^{-1}\ K^{-1}$
Density	7850	Kgm^{3}
Poisson Ratio	0.29	
Bulk Temperature	300	K
Young's modulus	219	GPa
Melting Temperature	1820	K

6.8 Result and discussion

Cutting force is considered as a crucial parameter in hard turning process which has a great impact on tool life, cutting temperature and machining precision. The distribution stress can be evaluated from the above figure.

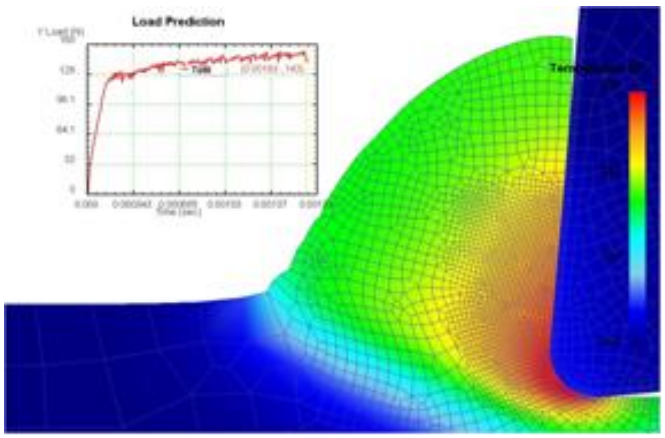

Figure 33 cutting force evolution obtained in simulation

In the beginning stage maximum force is generated at the tip of the cutting edge and decreased gradually.

The cutting force under a particular cutting depth was simulated. The finite element model results force was compared with the measured results and found to be in good correlation with an error percentage of 28%.

Chapter 7

Conclusion and Future Scope

7.1 Conclusion

The following outcomes are made using the present research work

1. The most favorable condition of cutting parameters as per full factorial design to minimize the tool wear surface roughness and force were concluded from above results. The optimum conditions are given below.
   - For force: 430rpm, 0.1 mm/rev, and 0.5mm depth of cut.
   - For surface roughness 710rpm, 0.15 mm/rev and 1mm depth of cut.
   - For tool wear 150rpm, 0.1 mm/rev and 1mm depth of cut.
2. The depth of cut is considered as the most significant factor which influences the performance characteristics with 45.71% contribution. The optimum process parameters obtained for all the three output responses combining using GRA is 150rpm speed, 0.1 feed rates and 0.5 depth of cut.
3. The finite element model results is compared with the measured results and found to be in good correlation with an error percentage of 28%.
4. The white layer thickness is mostly affected by tool flank wear (Tw) with increase in cutting velocity.

7.2 Scope for future work

1. Hard turning of experimental investigation on different types of hard materials can be carried out.
2. To determine the cutting temperature of hard turning operation by using FEM modeling process can be performed.
3. Micro hardness of the material which undergoes the formation of white layer can be measured and experimental verification can be executed.

References

1. Manoj Nayak and Rakesh Sehgal “Effect of tool material properties and cutting condition on machinability of AISI D6 steel during Hard turning” Arab j Science Engineering (2015) 40:1151-1164.
2. P.Kruth, L. Stevens, L. Froyen, B. Lauwers “Study of the white layer of a surface machined by die-sinking electro discharge machining” Annals of the CIRP 44 (1) (1995) 169-172.
3. Huang, Y. Liang, S.Y. Cutting force modeling considering the effect of tool thermal property application to CBN hard turning. Int j. Mach. Tool Manuf, 43(2003) 307-315.
4. G. Harinath Gowd, M Gunasekhar Reddy, Bathina Sreenivasulu “ Emperical modeling of hard turning process of Inconel using response surface methodology” Int. J of emerging technology and advanced engineering (2012) 2256-2459, volume2
5. B Fnides, M.A Yallese, T. Mabrouki, J. F Rigal “ Surface roughness model in turning hardened hot work steel using mixed ceramic tool” (2009) 1392-1207 Mechanika Nr.3 (77).
6. S. Abdul Kalam, A. Azad, M. Omkumar, Giri Sankar, R. Vajubunnisa Begum “ Elimination of white layer formation during Hard turning of AISI D3 Steel to improve fatigue life” IOSR journal of Mechanical and Civil Engineering (2015) 2278-1684
7. Ian S. Harrison “ Detecting white layer in hard turned components using nondestructive method” Thesis in Georgia Institute of Technology (2004)
8. G. Poulachon, A. Albert, M. Schluraff, I.S. Jawahir “ An experimental investigation of work material microstructure effects on white layer formation in PCBN hard turning” International Journal of Machine Tools & Manufacturing 45 (2005) 211-218
9. IIhan Asilyurk, Harun Akkus “Determining the effect of cutting parameters on surface roughness in hard turning using Taguchi method” Measurement 44(2011) 1697-1704.

10. Dong Min Kim, Vivek Bajpai, Hyung Wook " Finite Element Modeling of hard turning process via a micro-textured tool" International Journal of Advanced Manufacturing Technology (2015) 170-014-6747-X 78(9-12)
11. A. Ramesh, S.N. Melkote, L.F. Allard, L. Riester, T.R. Watkins " Analysis of white layer formation in hard turning of AISI 52100 steel" Material science and Engineering A 390 (2005) 88-97.
12. A. Aramcharoen, P.T. Mativenga " White layer formation and hardening effect in hard turning of H13 tool steel with CrTiAlN and CrTiAlN/MoST-coated carbide tools" Int. J Adv Manufacturing Technology (2008) 36: 650-657.
13. Manjunatha R, Umesh C K "Analysis and prediction of feed force, tangential force, surface roughness and flank wear in turning with uncoated carbide cutting tool using both Taguchi and Grey based Taguchi Method" Journal of multidisciplinary Engineering Science and Technology (JMEST) (2015) 3159-0040.
14. M. Dhanenthiran " An investigation of the effect of process parameters in turning operation on cast iron" SSRG International Journal of Mechanical Engineering (2016) (SSRG-IJME) volume3 Issue 2
15. M. Kaladhar, K. Venkata Subbaish, Ch Srinivas Rao and K. Narayana Rao " Optimization of process parameters in turning of AISI202 austenitic stainless steel" ARPN journal of engineering and applied sciences (2012) 1819-6068
16. Souad Makhfi, Raphael Velasco, Malek Habak, Kamel Haddouche, Pascal Vantomme "An optimized ANN approach for cutting forces prediction in AISI 52100 bearing steel hard turning". Science and Technology 3(1), 24-32.
17. G. Bartarya, S. K. Choudhury " Effect of tool wear on white layer thickness and sub surface hardness on hard turned EN31 steel" All India manufacturing technology , Design and Research conference (2014) IIT Guwahati.
18. D. Umbrello, L. Filice " Improving surface integrity in orthogonal machining of hardened AISI 52100 steel by modeling white and dark layers information" Manufacturing technology 58 (2009) 73-76.
19. Ashvin J. Makadia, J. I. Nanavati "Optimization of machining parameters for turning operations based on response surface methodology" Measurement 46 (2013) 1521-1529.

20. S.B. Salvi, R. R. Deshmukh, S.D. Deshmukh "Analysis of surface roughness in hard turning by using Taguchi method" International Journal of Engineering Science and technology (2013) 0975-5462 Vol. 5 No. 02
21. S.S Bosheh and P. T. Mativenga "White layer formation in hard turning of H13 tool steel at high cutting speed using CBN tooling" International journal of machine tools and manufacture 46.2 (2006) 225-233
22. S. R. Chauhan and Kali Dass "Optimization of machining parameters in turning of Titanium (Grade-5) alloy using Response surface methodology" Material and Manufacturing process (2012) 27:5 531-537
23. E. Aslan, N. Camuscu and B. Birgoren " Design optimization of cutting parameters when turning hardened AISI 4140 steel (63HRC) with Al_2O_3 + TiCN mixed ceramic tool Mater. Des, 28 (2007) 1618-1622.
24. M. C. Shaw and A.Vyas "The Mechanism of chip formation with hard turning steel" Annals of CIRP (1998) Vol. 47/1.
25. Mehdi Remadna and Jean Francois Rigal " Evolution during time of tool wear and cutting force in the case of hard turning with CBN inserts" Journal of Material Processing Technology 178 (2006) 67-75.
26. H. V. Ravindra, Y. G. Srinivasa and R. Krishnamurthy " Modeling of tool wear based on cutting forces in turning" Wear, 169 (1993) 25-32.
27. Li Qian and Mohammad Robiul Hossan " Effect on cutting force in turning hardened tool steels with cubic boron nitride inserts" Journal of Material Processing Technology 191 (2007) 274-278.
28. Z.C. Lin and D-Y Chen "A Study of cutting with a CBN tool" J. Mater. Process and Technology, 49 (1995) 149-164.
29. Saeed Zare Chavoshi and Mehdi Tajdari "Developed a surface roughness model in hard turning operation of AISI 4140 steel using CBN insert" Journal of material processing Technology 154 (2009) 87-93
30. Ibrahim A. AL-Zker "Fundamental of Hard turning process and the impact of CBN tool" Mater.Des 29 (2007) 1612-1618.
31. Zoltan Iosif Korka, Calin Octavian Miclosina and Vasile Cojocaru "An Experimental study of the cutting force in Metal Turning" ANUL XX, NR.2 (2013) 1453-7397

32. Moha Ashar, Ajitanshu Mishra Adnan Khan “Investigate the effect of machining hard turning process parameter on surface roughness of Cr-Mo alloy using Taguchi method” International Journal of Engineering Research Vol.3 Issue.6 (2015) 2371-7785
33. Nikolas. I. Galanis “Finite Element Analysis of the cutting forces in turning of Femoral Heads from AISI 316L stainless steel” World congress on Engineering (2014) 2078-0966
34. S.R, Deshmukh, B.K. Borkar. “ Tool life Analysis by using FEA of multilayer coated carbide insert., Int. j. of Engineering Research & Technology (JIERT), 2(6) (2013) 3408-3417.
35. Raczkovi, “ Tool life of cutting tool in case of hard turning” Hungarian J. of Indurstial Chemistry Veszprem, (38(2)2010) 133-136.
36. N. A. Talib, “Studying the effect of cutting speed and feed rate on tool life in turning process” Diyala j. of Engineering Science, (2010) 181-194.
37. A. K. Sahoo, T. Mohanty, “Optimization of multiple performance characterstic in turning using Taguchi’s quality loss function. An experimental investigation, Int. j. of Indurstial Engineering Computation, 4 (2013) 325-336.
38. Y. R. Bhoyar, P. D. Kamble, “Finite Element Analysis on temperature distribution turning process , Int. j. of Modern Engineering Research (IJMER), 3(1) (2013) 541-546.
39. J. Kopac, “Hardening phenomena of Mn-austenite steels in the cutting process” J. of Material Processing Technology, 109 (2001) 96-104
40. P. C. Sharma, Machining Fundamental and recent advances, 2008.